

Fluid Ejections in Nature

Elio J. Challita,^{1,2} Pankaj Rohilla,¹ and M. Saad Bhamla¹¹School of Chemical and Biomolecular Engineering, Georgia Institute of Technology, Atlanta, Georgia, USA; email: saadb@chbe.gatech.edu²George W. Woodruff School of Mechanical Engineering, Georgia Institute of Technology, Atlanta, Georgia, USA

ANNUAL REVIEWS CONNECT

www.annualreviews.org

- Download figures
- Navigate cited references
- Keyword search
- Explore related articles
- Share via email or social media

Annu. Rev. Chem. Biomol. Eng. 2024. 15:187–217

First published as a Review in Advance on April 26, 2024

The *Annual Review of Chemical and Biomolecular Engineering* is online at chembioeng.annualreviews.org<https://doi.org/10.1146/annurev-chembioeng-100722-113148>

Copyright © 2024 by the author(s). This work is licensed under a Creative Commons Attribution 4.0 International License, which permits unrestricted use, distribution, and reproduction in any medium, provided the original author and source are credited. See credit lines of images or other third-party material in this article for license information.



Keywords

organismal biophysics, physics of living systems, biofluid dynamics, fluid interfaces, nozzle, droplet, jets, bioinspired design

Abstract

From microscopic fungi to colossal whales, fluid ejections are universal and intricate phenomena in biology, serving vital functions such as animal excretion, venom spraying, prey hunting, spore dispersal, and plant guttation. This review delves into the complex fluid physics of ejections across various scales, exploring both muscle-powered active systems and passive mechanisms driven by gravity or osmosis. It introduces a framework using dimensionless numbers to delineate transitions from dripping to jetting and elucidate the governing forces. Highlighting the understudied area of complex fluid ejections, this review not only rationalizes the biophysics involved but also uncovers potential engineering applications in soft robotics, additive manufacturing, and drug delivery. By bridging biomechanics, the physics of living systems, and fluid dynamics, this review offers valuable insights into the diverse world of fluid ejections and paves the way for future bioinspired research across the spectrum of life.

1. OVERVIEW AND MOTIVATION

Fluid transport is a biological imperative. Living organisms pump fluids, either internally or externally, to conduct essential functions vital to their survival and proliferation. This capacity has evolved in diverse ways across kingdoms and taxa, encompassing plants, fungi, and animals. Fluid ejection, the main focus of this review, is a distinct yet integral part of fluid transport (2, 3). Despite having important ecological, morphological, and evolutionary consequences, it has received limited attention (4–6).

The complexity and diversity of fluid ejections across organisms stem from an intricate interplay between fluid dynamics and biological function. Each species has evolved unique mechanisms to utilize fluid ejections for particular needs. These mechanisms are bounded by the physical laws governing the world they inhabit and the properties of the fluids they handle.

In this review, we develop a framework for understanding fluid ejections across various organisms and contexts (**Figure 1**). While we present a wide array of biological fluid ejections, our goal is not to provide a comprehensive overview. Instead, we focus on rationalizing the sheer diversity of fluid ejections in terms of (*a*) the organisms involved (from fungi to whales), (*b*) the biological functions served (e.g., excretion, hunting, defense, predation, dispersion), (*c*) the mechanisms utilized (catapulting, pumping, destructive), (*d*) their physical and temporal scales (microns to meters, milliseconds to seconds), and (*e*) fluid characteristics (e.g., viscoelasticity, adhesion, chemical reaction). We pay particular attention to how biological organisms contend with fluid forces across physical scales, concentrating on identifying dominant forces through nondimensional numbers and analyzing how these forces shape the ejected fluids. In some cases, we offer preliminary quantitative and order-of-magnitude analyses and hypotheses in areas where fluid ejections are understudied or not fully understood. We exclude certain topics like anatomy and the evolutionary history of fluid ejections from the scope of this review. We hope that biologists, especially those interested in organismal biofluid transport, as well as physicists and engineers seeking to apply these principles to engineering challenges, will find this examination resonant.

2. FUNDAMENTALS OF NEWTONIAN FLUID EJECTION

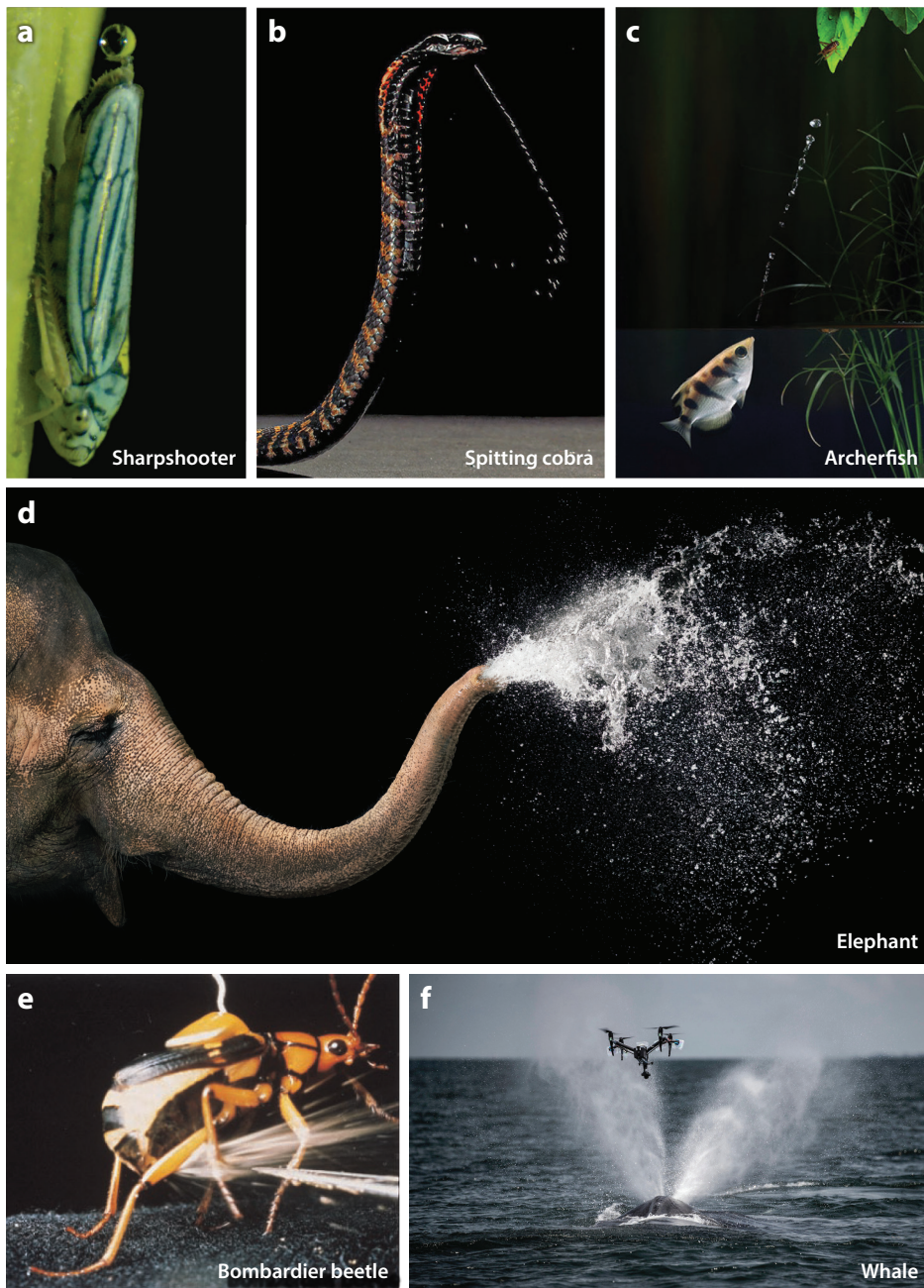
Fluid ejection describes the process where a stationary fluid within a pipe begins to move and eventually exits through an orifice (nozzle). The shape of the exiting fluid depends on the dominant hydrodynamic forces, fluid properties, flow speed, and geometric/mechanical properties of the pipe/nozzle. The study of fluid dynamics of fluid ejections has been a subject of fascination throughout history, captivating scientists and engineers alike (**Supplemental Figure 1**). This study dates back to Leonardo da Vinci's examinations of jet behavior and fluid cohesion's role in drop formation (9) (**Supplemental Figure 2**). Recent studies have further outlined fluid ejection fundamentals through an orifice, focusing on jetting and breakup phenomena across scales (10–12).

Consider a Newtonian fluid of density ρ , with viscosity μ , flowing through a circular cylindrical nozzle of length l and a diameter d at speed \mathbf{u} , under gravitational acceleration g . We assume a rigid, smooth cylinder with no corrugations and stagnant surrounding air (no wind flow or external perturbations) (**Figure 2b**).

The Navier–Stokes equation, essentially the continuum version of Newton's second law of motion, describes the fluid's motion:

$$\rho \left(\frac{\partial \mathbf{u}}{\partial t} + \mathbf{u} \cdot \nabla \mathbf{u} \right) = -\nabla p + \mu \nabla^2 \mathbf{u} + \mathbf{F}_{\text{external}}$$

Within the nozzle, inertial forces arise from the fluid's mass and acceleration, and viscous forces relate to the fluid's inherent resistance to flow and friction with the walls. At the fluid–air interface, surface tension γ arises due to the imbalance of intermolecular attractions. Since our focus is on the specific air–liquid interface, we exclude complex fluid–fluid interfaces (13) and fluidic jets formed



(Caption appears on following page)

Figure 1 (Figure appears on preceding page)

Fluid ejections in nature. Fluid ejection spans multiple scales and species, taking different forms for various functions. (a) A blue-green sharpshooter (*Graphocephala atropunctata*) excretes droplets one at a time. Panel reproduced with permission from Reference 4. (b) A ring-necked spitting cobra (*Hemachatus* sp.) spits a stream of venom in self-defense. Panel reproduced with permission from the Trustees of the Natural History Museum. (c) An archerfish (*Toxotes* sp.) expels a fluid stream to hunt insects lying on leaves. Panel reproduced with permission from Scott Lindstead. (d) An elephant (Elephantidae) sprays water out of its trunk for bathing or cooling. Panel reproduced with permission from Tim Flach. (e) A bombardier beetle (*Stenaptinus insignis*) expels a spray of chemicals for self-defense. Panel reproduced with permission from Reference 7. (f) A humpback whale (*Megaptera novaeangliae*) expels a burst of air and water jet through its blowhole as part of its breathing process. A snotbot drone (8) collects fluidic samples of a humpback whale's liquid sput. Panel reproduced with permission from Reference 8.

in other viscous fluids, such as those in underwater propulsion by insect larvae, cephalopods, and other marine creatures, from the scope of this analysis (14). Surface tension forces influence droplet formation and fluid jet behavior, especially at small scales (15). The normal stress balance at a free surface must be balanced by the curvature pressure associated with surface tension: $\mathbf{n} \cdot \mathbf{T} \cdot \mathbf{n} = \gamma(\nabla \cdot \mathbf{n})$, where \mathbf{n} is the unit normal to the surface and $\mathbf{T} = -p\mathbf{I} + \mu[\nabla \mathbf{u} + (\nabla \mathbf{u})^T]$ is the stress tensor and p is the pressure (16). External forces such as gravity, represented by $\mathbf{F}_{\text{external}}$, also affect fluid flow, particularly at larger scales. In summary, fluid forces can be categorized as bulk (viscosity, inertia), interfacial (surface tension), or external (gravitational), i.e.,

$$\mathbf{F}_f = f(\mathbf{F}_v, \mathbf{F}_\mu, \mathbf{F}_\gamma, \mathbf{F}_g).$$

To assess the relative magnitudes of these forces, we consider several dimensionless numbers, including Bond number (Bo), Weber number (We), Reynolds number (Re), Ohnesorge number (Oh), and Froude number (Fr), in the sidebar titled Dimensionless Numbers for Newtonian Liquids in Air. Within the context of our initial assumptions, the relative magnitudes of hydrodynamic forces determine the fluid's shape exiting a nozzle. This represents a simplified model, as many biological organisms exhibit more complex characteristics such as non-Newtonian behavior, viscoelasticity, internal corrugation, noncylindrical geometries, and flexible or active nozzles (discussed in Sections 4 and 5).

3. REGIMES OF NEWTONIAN FLUID EJECTIONS

Building on the fundamental understanding of nondimensional numbers presented in the sidebars titled Dimensionless Numbers for Newtonian Liquids in Air and Dripping and Jetting Regimes for Newtonian Fluids, we now present a comprehensive framework that leverages Bo and We to categorize fluid ejection phenomena (Figure 3). This framework provides a map comprising four distinct quadrants, each illustrating the dominance of specific forces, including inertia, gravity, and surface tension. For these calculations, we use the nozzle diameter as the characteristic length (and not the size of the organism) and the average speed of the effective speed of the exiting fluid. Note that since not all nozzles in biological systems are circular, the hydraulic diameter may be used to estimate the effective diameter $d = 4A/P$, where A is the area of the nozzle and P is the perimeter of the nozzle.

The relationship between We and Bo serves as a critical tool to capture both the scale and the speed of the exiting fluid. It allows us to delineate the underlying behavior, function, mechanism, and governing fluid principles that dictate how organisms eject fluids within specific We - Bo quadrants. It is essential to recognize that the demarcations at $Bo = 1$ and $We = 1$ are not rigid boundaries but rather indicative markers to underscore the prevailing forces. The actual transition between quadrants is more nuanced, with unity presented here only as an intuitive heuristic. Some references, especially in engineering applications, define jetting when $We > 8$ (17).

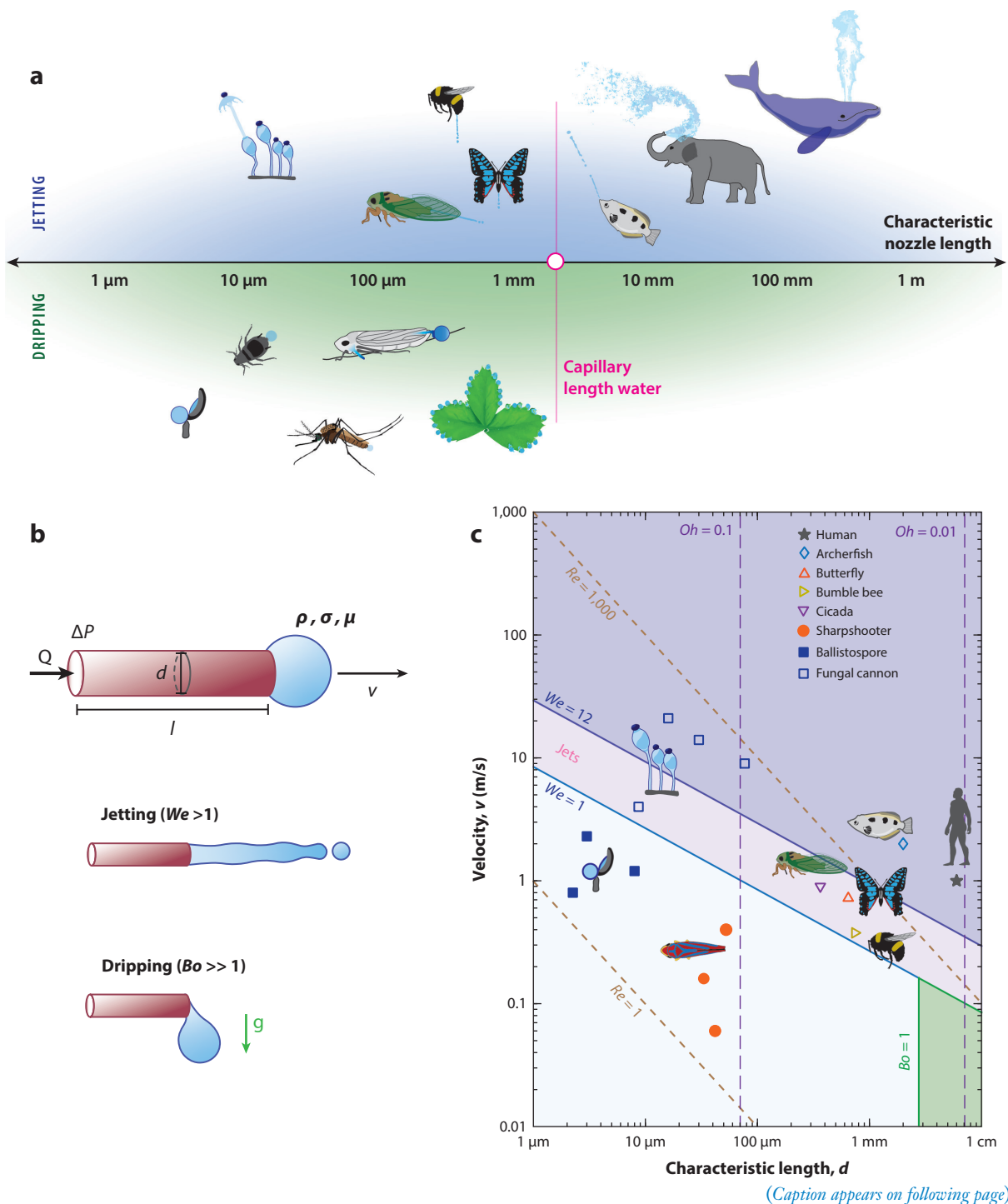


Figure 2 (Figure appears on preceding page)

Biological fluid ejection: dripping to jetting. (a) Biological organisms across various taxa and length scales in nature eject fluids, which can be categorized as dripping or jetting. (b) The fluid dynamics of fluid ejection is evaluated by considering the fluid flow of a Newtonian fluid within a smooth, rigid, cylindrical pipe. The fluid exhibits dripping when surface tension forces are dominant at $Bo < 1$ $We \ll 1$ and exhibits jetting when inertial forces or gravitational forces are at high $We \gg 1$. (c) Considering water as the fluid flow with a speed v out of an orifice with a characteristic length (diameter) d . The lines correspond to the following dimensionless numbers, Bond number $Bo = \rho gd^2/\gamma$, Weber number $We = \rho v^2 d/\gamma$, Ohnesorge number $Ob = \mu/\rho dy$, and Reynolds number $Re = \rho vd/\mu$, reflecting the interplay of surface tension and gravitational, inertial, and viscous forces. The highlighted areas reflect the different solutions and the various fluid regimes, including dripping and jetting.

DIMENSIONLESS NUMBERS FOR NEWTONIAN LIQUIDS IN AIR

The following dimensionless numbers are essential for characterizing Newtonian fluid ejection phenomena in air, where v is the 1D fluid speed at the nozzle exit, d is the diameter of the nozzle, l is the length of the tube, ρ is the fluid density, g is the gravitational acceleration, γ is the surface tension, and μ is the fluid viscosity:

$$\text{Bond number } (Bo) : \frac{\text{gravity}}{\text{surface tension}} = \frac{\rho gd^2}{\gamma},$$

$$\text{Weber number } (We) : \frac{\text{inertia}}{\text{surface tension}} = \frac{\rho v^2 d}{\gamma},$$

$$\text{Reynolds number } (Re) : \frac{\text{inertia}}{\text{viscous forces}} = \frac{\rho vd}{\mu},$$

$$\text{Ohnesorge number } (Ob) : \frac{\text{viscous forces}}{\sqrt{\text{surface tension} \cdot \text{inertia}}} = \frac{\mu}{\sqrt{\rho \gamma d}} = \frac{\sqrt{We}}{Re}, \text{ and}$$

$$\text{Froude number } (Fr) : \frac{\text{inertia}}{\text{gravity}} = \frac{v^2}{gl}.$$

DRIPPING AND JETTING REGIMES FOR NEWTONIAN FLUIDS

A Newtonian fluid exiting a nozzle into the air can be divided into two main regimes: dripping and jetting, characterized by the Bond number (Bo) and the Weber number (We) (Figure 2).

Dripping Regime $Bo < 1$ and $We < 1$

The fluid exits in droplet form, growing slowly before detaching at a critical size. Gravity plays a significant role in droplet breakup, producing large constant-mass droplets at a slow rate (Figure 2a,b).

Jetting Regime $We > 1$

As the exiting fluid's speed increases, inertial forces overcome surface tension, transitioning into jetting. Various behaviors emerge, including periodic, chaotic dripping ($1 < We < 8$) and a continuous stream of fluid jetting at higher We values (Figure 2a,b).

Breakup Regimes $We \gg 1$

In jetting, jet dynamics are sensitive to mechanical perturbation or thermal excitation. A small disturbance will grow when its wavelength exceeds the jet's circumference, leading the fluid to break up into droplets. Different jet breakup

(Continued)

(Continued)

regimes can be identified on the basis of the Ohnesorge number (Ob) and the Weber number for liquid (We_L) and gas (We_g) (17). Jet breakup regimes are not the focus of the review and are presented in the **Supplemental Material** and **Supplemental Figure 3**.

Ohnesorge Number: Viscosity and Inertio-Capillary Breakup

The Ohnesorge number (Ob) sheds light on the stability and breakup of a liquid jet, as well as on the formation of satellite droplets. At $Ob \ll 1$, a fluidic jet lies in the inertio-capillary regime, where it may break quickly into smaller satellite droplets due to the combined effects of inertia and surface tension. At $Ob > 1$, or at $d < 10^{-8}$ m for water, viscous forces become relevant in jet dynamics. Formed jets break up faster due to viscous forces.

Froude Number: Gravity and Inertia

The Froude number (Fr) evaluates the relative magnitude of inertia over gravitational effects in fluid jets. A classic example of a low Fr is the falling jet stream driven by gravity. Alternatively, a jet with high initial velocity results in a significantly high Fr .

3.1. Surface Tension Regime: $Bo < 1$, $We < 1$

In this regime, surface tension dominates, leading to the characteristic dripping of fluids. The cohesive forces of surface tension form droplets and make them adhere to hydrophilic surfaces through capillary adhesion (15, 18). Such adhesion may cause droplets to remain attached to the nozzle's tip, hindering their ability to detach (19). This phenomenon is particularly pronounced for micrometer- to millimeter-scale organisms, whose size is comparable to or smaller than the capillary length l_c . In this context, surface tension forces can be substantial relative to the organism's size and weight, even to the point of trapping and endangering tiny organisms (20–22).

Various organisms have evolved innovative strategies to counter these forces. Since fluidic pumping is insufficient for droplet removal, strategies incorporate secondary mechanisms tailored to counteract capillary adhesion. These methods exploit the inherent properties of surface tension. Some strategies, for example, leverage the elastic properties of surface tension to use it as an engine for fluid ejection [e.g., superpropulsion in sharpshooters (4) (**Figure 4a,b**), droplet coalescence in ballistospores (23) (**Figure 4b–j**), and kicking in free aphids (24)]. Others reduce the effect of surface tension altogether by coating the droplets with a hydrophobic layer [e.g., hydrophobic waxing in gall aphids (24) (**Figure 4c,d**)]. Some organisms even rely on symbiotic relationships with external agents, such as ants, to remove the excreted fluids (24). Organisms such as some mosquito species exploit capillary adhesion to retain the droplets for evaporative cooling, a process that, while distinct, shares the underlying principle of evaporation with the cooling mechanism in mammals through sweating, where sweat glands release fluid that evaporates from the skin's surface to reduce body temperature (25) (**Figure 4f,g**).

3.1.1. Excretion in sap-feeding insects: kicking, catapulting, pinching, and waxing. Sap-feeding insects (hemipterans) are among the most extreme biological pumps (18). They subsist on a liquid diet of plant fluids, using specialized stylets to extract plant sap from phloem and/or xylem tissues (31). With high rates of fluid consumption and extended feeding periods at specific sites, these insects generate significant volumes of liquid waste at singular locations. Fluid ejection

Supplemental Material >

Superpropulsion: a phenomenon in which an elastic projectile (e.g., water droplet) may be ejected at a speed higher than that of the actuator through temporal tuning

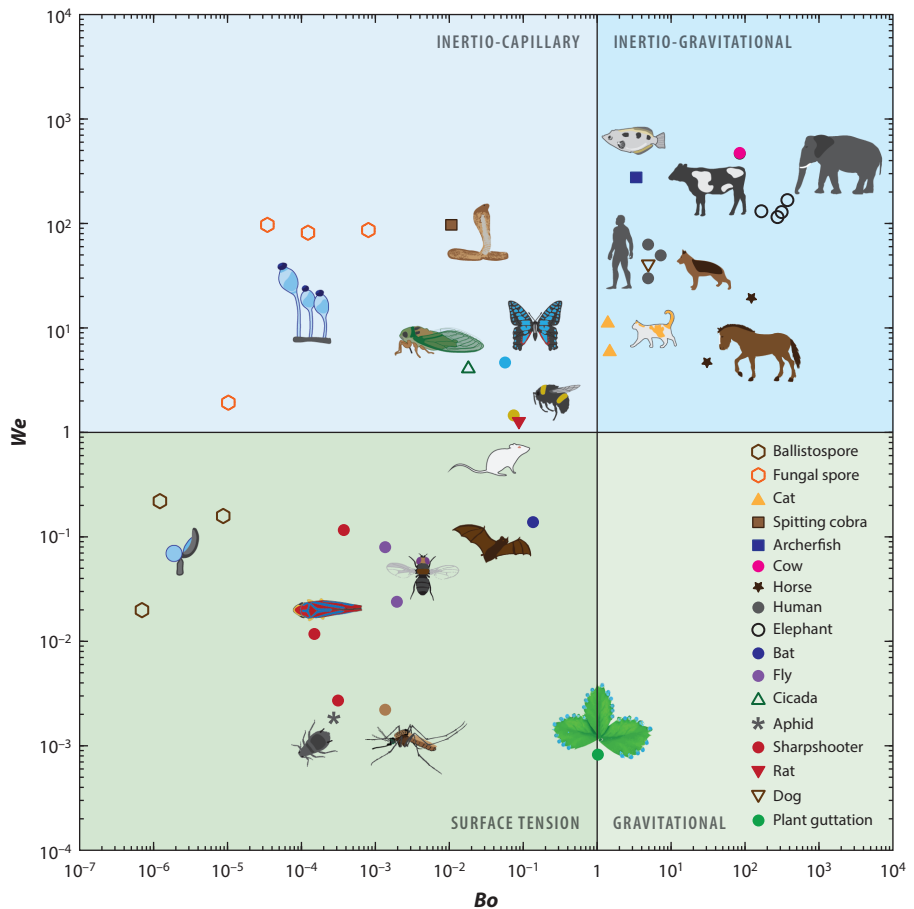


Figure 3

Mapping Newtonian fluid ejections via a Bond (Bo) and Weber (We) numbers framework. This framework identifies four quadrants to highlight the interaction of surface tension, inertia, and gravity, ignoring the effect of viscous forces [Ohnesorge number (Ob) $\ll 1$] (see the full list in **Supplemental Table 1**). In the surface tension regime ($Bo < 1, We < 1$), surface tension dominates, causing fluids to exit the nozzle as droplets. In the inertio-capillary regime ($Bo < 1, We > 1$), fluid ejections form jets influenced by inertial forces and surface tension. The inertio-gravitational regime ($Bo > 1, We > 1$) corresponds to ejections where inertia and gravity (hydrostatic pressure) cause fluids to exit as jets through a larger nozzle, as seen in urination in most large mammals. The gravitational regime ($Bo > 1, We < 1$) is characterized by gravity slowly driving the dripping of a fluid. For plant guttation, a droplet grows, reaching a critical weight, before rolling over. (Considering the size of the droplet as characteristic length, Bo is used here.)

becomes crucial for maintaining hygiene, fostering symbiotic relationships, and distancing from waste to deter predators (6).

Xylem-feeding insects such as sharpshooters consume vast quantities of xylem sap, approximately 300 times their body weight per day (6). They expel liquid waste using a specialized appendage called the anal stylus (anal ligulae), forming a water droplet within 80 ms and then catapulting it at 14 g (4) (**Figure 4a,b**). These insects exploit the elastic properties of droplets to eject fluidic droplets, using surface tension as a Hookean spring to elastically deform the droplets during catapulting (32, 33). By tuning the frequency of their anal stylus (the actuator) to match

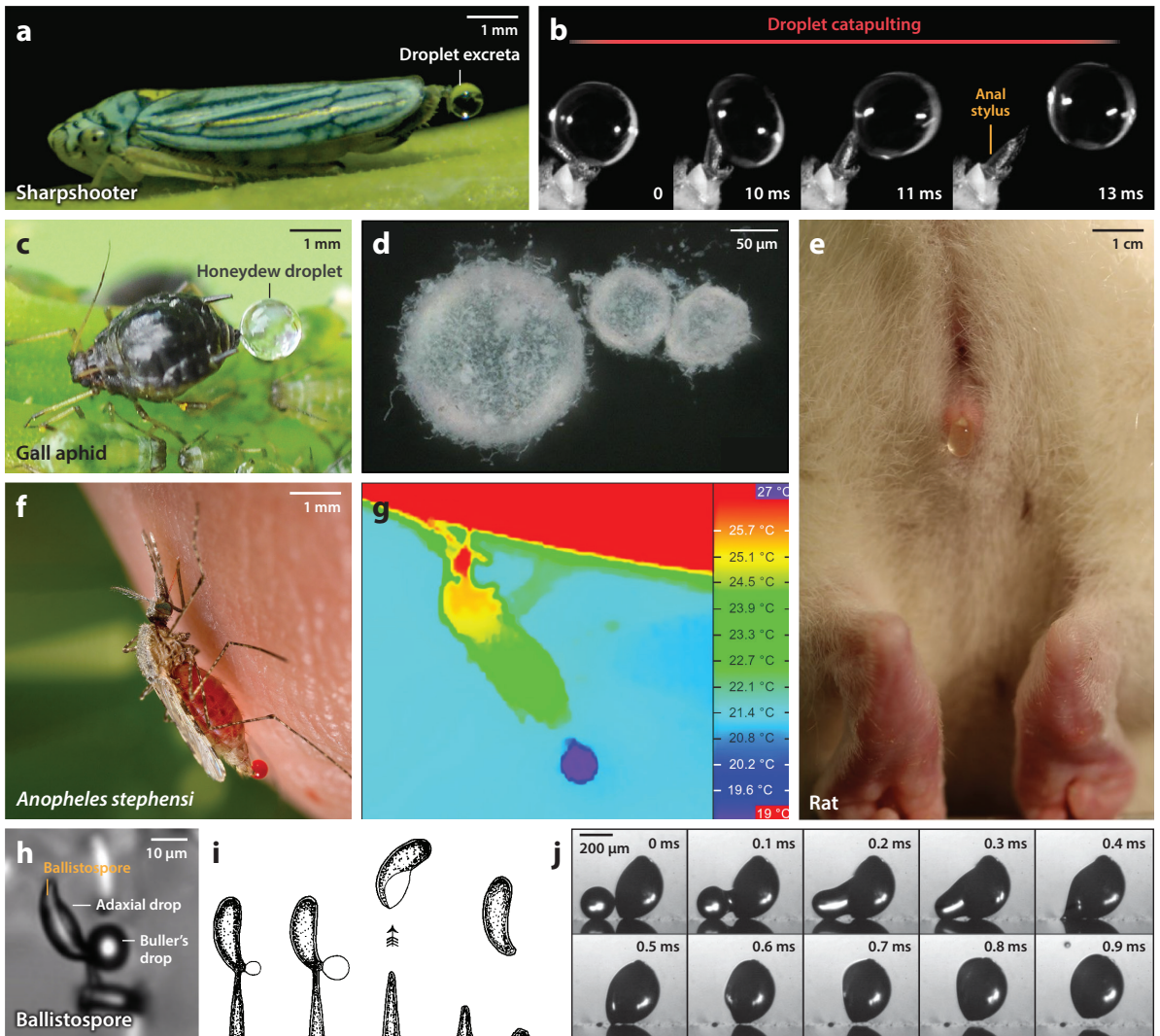


Figure 4

Exploring the surface tension regime: a diversity of fluid ejections. (a) A blue-green sharpshooter (*Graphocephala atropunctata*) feeds on a basil leaf and excretes droplet excreta. Panel reproduced with permission from Reference 4. (b) Collage showcasing the ultrafast droplet-caterpulting mechanism used by glassy-winged sharpshooters (*Homalodisca vitripennis*). Surface tension mediates the droplet's deformation due to its elasticity. Panel reproduced with permission from Reference 4. (c) A galling aphid (*Aphis* spp.) excretes a honeydew droplet. Panel adapted from Amada44/Wikipedia (2011) (CC BY 4.0). (d) Aphids secrete powdery hydrophobic wax that coats the sugar-rich droplet to form a liquid marble, enabling easy rolling. Panel adapted with permission from Reference 26. (e) A Wistar rat (*Rattus norvegicus*) urinates a droplet. Panel adapted with permission from Reference 5. (f) A mosquito (*Anopheles stephensi*) projects a blood-rich droplet for thermoregulation. (g) Thermographic image of an *A. stephensi* mosquito feeding on an anesthetized mouse. The mosquito cools itself through evaporative cooling; it retains a fluid droplet at the abdomen's end, causing a temperature gradient along its body. Panel adapted with permission from Reference 27. (h) Ballistospore of *Tilletia caries* moments before discharge via coalescence between the Buller's drop and the adaxial drop. Panel adapted with permission from Reference 28. (i) Buller's 1922 illustration of the discharge of spore and fluid droplet in *Calocera cornea*. Panel adapted with permission from Reference 29. (j) Experimental demonstration of a ballistospore-inspired launch of a spore-shaped polystyrene particle from a flat superhydrophobic substrate following the coalescence of two inkjet-printed drops. Panel adapted with permission from Reference 30.

the Rayleigh frequency of their elastic droplets, they efficiently remove fluidic excreta using super-propulsion (4, 34). The stylus's surface also exhibits parahydrophobic properties, enabling droplet adherence for control while maintaining a high contact angle for easy removal (35).

Sharpshooters catapult discrete water droplets rather than expel continuous fluid jets because of two primary energetic constraints: (a) their nutrient-scarce diet, which consists of ~95% water, and (b) the negative pressure of the xylem sap. Consequently, sharpshooters expend significant energy to pump this fluid using their cibarial muscles, extracting only a small amount of nutrients (36). Such dietary and fluid mechanics considerations point to energetic constraints related to fluidic pumping at their small scale (37).

The energetics of excretion can be assessed by calculating the pressure P required for pumping droplets generated by the constriction dynamics of circular muscles located in the insect's hindgut (38). To effectively eject fluid, this pressure P must overcome combined viscous forces ($F_\mu \propto \mu lu/d^2$) and surface tension forces ($F_\gamma \propto \gamma/d$). As the diameter d becomes smaller, the overall pumping pressure increases, revealing that the pressure needed for droplet formation is notably lower—specifically four to eight times lower—than that needed for a continuous jet $We > 1$.

From an energetics standpoint, jetting out fluid waste, compared with forming and catapulting droplets, could lead to a net energetic deficit in these sharpshooters (4, 36). This underscores the energetic advantage of the droplet ejection mechanism over jetting, especially at the microscale. However, ejecting droplets via catapulting becomes increasingly challenging as droplet size decreases. Smaller droplets require a greater minimum acceleration for propulsion, as they are harder to deform due to higher internal pressure ($P \propto \gamma/d$). Therefore, the critical acceleration required for droplet detachment scales as $D^{-3/2}$, where D is the droplet diameter (39). Such dynamics impose constraints on the capacity of biological actuators to achieve the necessary acceleration for smaller droplet detachment. This constraint may explain why sharpshooter nymphs, which are typically smaller than adults, utilize a droplet ejection mechanism based on droplet pinching, a subject currently under investigation.

Phloem-feeding insects such as aphids face different challenges. Their excreted fluid, called honeydew, is rich in sugar (Figure 4c). The accumulation of honeydew could foster detrimental fungi or parasites and signal their location to predators (40, 41). Aphids, especially those that exhibit site fidelity, have evolved remarkable adaptations to manage their liquid waste. Galling aphids, for example, coat their honeydew with a hydrophobic powdery wax (Figure 4d) to form a liquid marble that rolls away from their bodies, averting build-up and ensuring hygiene (24, 41, 42). Free-living aphids resort to kicking fluids away (43) or establishing symbiotic relationships with ants. Spotted lanternflies (*Lycorma delicatula*), another phloem-feeding insect species (44), expel fluidic honeydew droplets using a currently unknown catapulting mechanism.

3.1.2. Fungal ballistospores: spore ballistics through droplet coalescence. Numerous fungal species use surface energy properties to explosively release their ballistospores (Figure 4b–j). This impulsive movement is mediated by surface tension, where potential energy stored in two separate droplets is released via coalescence. This coalescence occurs between a spherical Buller's drop at the spore's hilar appendix and a flattened drop on the spore's adaxial side (23, 45). Ballistospores achieve remarkable launch dynamics, with initial velocities estimated at ~1 m/s, although their range is limited to ~100 μm due to viscous drag. The ejection mechanisms are single-shot and destructive, with each spore undergoing one impulsive movement for dispersion. From an engineering standpoint, coalescence-induced jumping has potential applications in self-cleaning, anti-icing, antifrosting, and enhancing condensation heat transfer (30, 46).

3.1.3. Small mammals: droplet excretion mechanisms. Fluid dynamics principles in excretion extend to small mammals as well. The law of urination in mammals states that urination time

is length scale invariant, with mammals urinating in jets within 21 ± 13 s (5). However, small mammals weighing less than 3 kg, such as rodents (bats, rats, and mice) (**Figure 4e**), typically release excrement as individual droplets or weak jets that break up immediately due to the Rayleigh–Plateau instability ($We \sim 1$). Equalizing the bladder pressure required to overcome surface tension forces reveals a limit in orifice diameter of ~ 100 μm in mammals below which excretion in the form of continuous jets is impossible (5). This constraint does not apply to arthropods such as butterflies, cicadas, and bees, which can form jets even at smaller scales (discussed in Section 3.2.2). Larger bat species, such as the flying fox (*Pteropus* spp.), are also documented to release their urine in jets, further supporting the notion that the ability to form continuous jets is determined not solely by size but also by other morphological and biological factors. This observation underscores deeper morphological differences between mammals and arthropods and highlights the complexity of fluid dynamics in biological systems that warrants further study.

3.1.4. Evaporative cooling in arthropods: thermoregulation through excreted drops. Thermoregulation is vital for all organisms, especially for arthropods feeding on warm-blooded hosts or sugary solutions. These species have developed complex adaptations to manage excessive heat, including evaporative cooling. During this process, phase changes like evaporation require latent heat, producing a cooling effect on the evaporating fluid and its surroundings.

Hematophagous species such as mosquitoes and sand flies excrete fluid droplets during blood feeding. *Anopheles* mosquitoes, for example, reduce their internal temperature by excreting and retaining fluid droplets at their abdomen's end (27). The subsequent evaporation significantly cools the mosquito's body (**Figure 4f,g**). Species that do not retain the fluid droplet appear to lack this thermoregulatory ability (27).

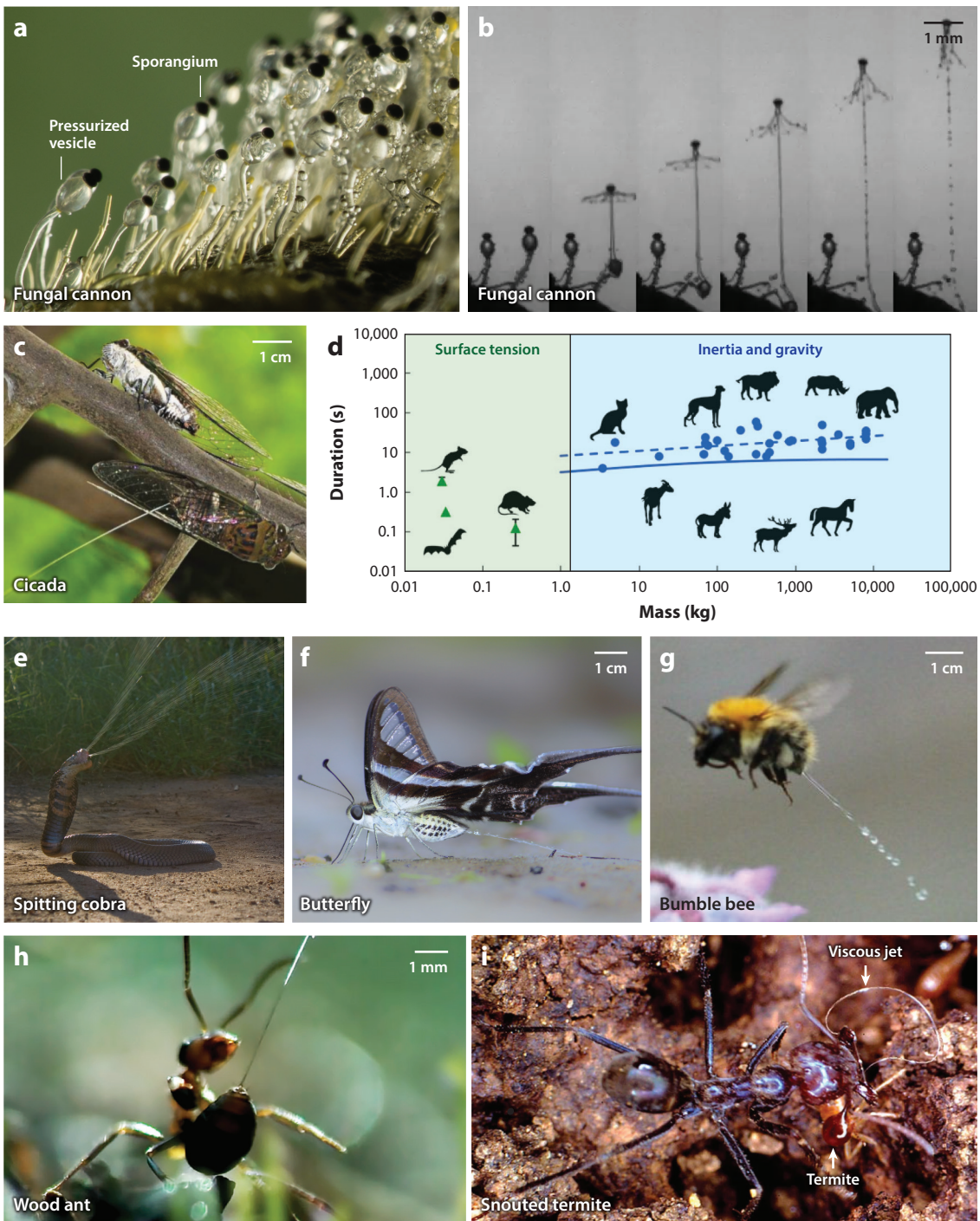
Honey bees and bumble bees also exhibit thermoregulation through fluid ejection (47, 48). They regurgitate a droplet of nectar through their mouthparts to cool their heads, maintaining the brain's functional temperature range. This adaptation prevents overheating in hot climates or during strenuous activities such as flying and foraging.

Other observed thermoregulatory mechanisms extend beyond hematophagous species. Grasshoppers that feed on succulent plants, sphinx moths (49), and cicadas (50) employ similar strategies to exude fluids for body heat regulation, although the specific details require further investigation. In mammals, evaporative cooling is achieved through sweating, with specialized sweat glands releasing sweat through pores ~ 60 – 80 μm in diameter (in humans). Unlike forceful expulsion, the sweat fluid is released gradually, facilitated by the body's heat and the evaporation process itself.

3.2. Inertio-Capillary Regime: $Bo < 1$, $We > 1$

In the inertio-capillary regime, where $Bo < 1$ and $We > 1$, inertia dominates, and surface tension plays a significant role over gravitational force (**Figure 5**). Within this regime, the Ob (see the sidebars titled Dimensionless Numbers for Newtonian Liquids in Air and Dripping and Jetting Regimes for Newtonian Fluids) determines the dynamics of jet breakup, but we restrict our studies to the limit where $Ob < 1$. For $Ob \sim 1$, the case for highly viscous fluids or very small nozzle size, fluids may become too viscous to be jettable (51).

Small organisms face challenges in creating fluid jets: The pressure required to drive fluid flow increases due to viscous forces ($F_{\text{viscous}} \propto u/d^2$) and surface tension ($F_{\text{surface tension}} \propto 1/d$) (4, 5). Despite these challenges, several advantages exist for small organisms in creating jets. High-speed jets enable organisms to discharge fluids at specific targets quickly, serving defensive or offensive purposes [e.g., red wood ants (*Formica rufa*) (53), *Nasutitermes* termites (59), and spitting cobras (*Naja mossambica*) (54)] or high-acceleration release of spores [e.g., fungal cannons



(Caption appears on following page)

Figure 5 (Figure appears on preceding page)

Inertio-capillary ejections across species ($Bo < 1$, $We < 1$). (a) A cluster of fungal cannons (*Pilobolus crystallinus*) before they explosively launch their spores. A vesicle generates pressure to eject the spore at up to 20,000 g. Panel adapted with permission from Sava Krstic/Wikipedia (https://en.wikipedia.org/wiki/Pilobolus_crystallinus) (CC BY-NC-SA 3.0). (b) Sequence of the spore ejection of *Pilobolus kleinii* (52). (c) *Cyrtosticta umbrosa* cicadas feed and urinate on a leopard tree (*Libidibia ferrea*) at the Labrador Nature Reserve, Singapore. Panel adapted with permission from Tzi Ming Leong. (d) The law of urination shows that mammals with a mass greater than 3 kg urinate in jets within 21 ± 13 s, while smaller mammals such as rodents urinate in singular droplets. This law does not apply to smaller insects such as cicadas, which can urinate in powerful jets despite their smaller size (~ 5 g). Panel adapted with permission from Reference 5. (e) A Mozambique spitting cobra (*Naja mossambica*) spits a large venom jet in self-defense. Panel adapted from Steven Gilham/Flickr (2010) (CC BY-NC 2.0) (f) A white dragontail butterfly (*Lamproptera curius*) emits a stream of urine. Panel adapted from Subhendu Khan (CC BY 4.0). (g) A bumble bee (*Bombus* sp.) emits a fluid jet midair. Panel provided by Mark Parrot and SWNS.com. (h) A red wood ant (*Formica rufa*) emits a jet of formic acid from its abdomen tip. Photo provided by Terra Mater Studios. (i) A snouted termite (*Nasutitermes exitiosus*) spits a viscous jet against a larger ant predator (*Iridomyrmex purpureus*). Panel provided by Tom Eisner.

(52)]. Additionally, higher-speed jets imply a higher flow rate, allowing the discharge of more fluid within a given time frame. This capability is potentially beneficial for organisms such as cicadas, which must process large volumes of low-energy-nutrient xylem sap to extract sufficient nutrients (55).

3.2.1. Arthropods: jetting chemicals for survival. Many arthropods, including *Formica rufa* (red wood ant or horse ant), have evolved to discharge jets of chemicals for defense or predation. *F. rufa* worker ants release a precise jet of formic acid from their abdomen, covering distances of several centimeters (Figure 5b). This acid accounts for up to 20% of their body weight (53). The production and storage of this acid occur in venom glands within the gaster. The acid is released through an acidopore located at the abdomen's tip. Similar behavior is observed in other ant species, such as yellow crazy ants (*Anoplolepis gracilipes*) and tawny crazy ants (*Nylanderia fulva*). However, the fluid dynamics governing the projection of formic acid remain not fully understood. This lack of understanding is not surprising, considering the inherent challenges and potential dangers of filming high-speed acid jets up close. Our personal attempts to capture these phenomena have underscored the complexity and risk involved. Given the fluid properties of formic acid ($\gamma = 37$ mN/m, $\mu = 1.78$ mPa·s, $\rho = 1220$ kg/m³) and the size of the acidopore of $d < 100$ μm, we estimate their fluid ejection to be $We \sim \mathcal{O}(100)$.

Conehead termites (*Nasutitermes* spp.) have also evolved jet-spitting behavior for defense (56, 57) (Figure 5i). The soldier caste of these termites squirts viscous jets from a nozzle-like head projection, termed the nasus, toward perceived danger. The defensive substance serves a dual purpose: It immobilizes smaller attackers and deters larger threats (58). The jets achieve speeds of $u \sim 0.4$ m/s within $t \sim 250$ ms, extending almost two times the ant's body length and forming liquid-like lassos that can physically entrap large predatory ants (59).

3.2.2. Cicadas: powerful fluidic jets in xylem sap-feeders. Species of cicadas from the Amazon and Southeast Asia produce a range of fluidic jets. Cicadas, given their larger size, have fluidic capabilities distinct from those of sharpshooters, another type of insect that feeds on xylem sap (60) (see discussion in Section 3.1.1) (Figure 5c,d). Unlike sharpshooters, cicadas outmaneuver the inertio-capillary regime, generating fluidic jets with $We \sim 2$. This capability could be linked to their need to digest vast amounts of xylem sap fluid to extract sufficient nutrients. However, a comprehensive understanding of the energetics encompassing feeding, nutrient extraction, and excretion in cicadas remains unexplored. The study of cicadas has been further complicated by their varied breeding times, with some species emerging annually while others have life cycles spanning several years. The extreme difficulty in lab-rearing them has also hindered research, and to date, no one has successfully cultured cicadas in a laboratory setting (60).

Rheology: the study of the deformation and flow of matter, encompassing both Newtonian and non-Newtonian behaviors

3.2.3. Fungi and citrus: explosive fluid jets. Many fungal species, including those of the phyla Ascomycota, Zygomycota, and Entomophthoromycota, rely on a fracture release mechanism to disperse their spores (61). This process begins with water absorption into a specific chamber through osmosis, leading to an impulsive jet release when the pressure reaches a critical level (0.31–1.54 MPa).

In ascomycetes, the fluid-filled chambers, termed asci, contain osmolytes that trigger an influx of water before discharging with the spores. *Gibberella zeae* has the fastest launch acceleration and velocity at 870,000 g and 34.5 m/s, respectively (52) (**Figure 5a,b**). *Ascobolus immersus* and the spitting fungus *Glomerobolus gelineus* achieve launch distances of ~0.3 m, sufficient to reach the turbulent boundary layer for wind dispersal (52, 62). The aerodynamic shape of the spores minimizes energy loss and drag during ejection, extending distance and reach. Ascomycetes eject spores collectively, and their synchronicity enhances dispersion, allowing spore launches to achieve distances 20 times greater than those of individual spores (63).

Pilobolus (Zygomycota), known as the squirt-gun, hat thrower, or fungal cannon, thrives on herbivore dung. It forms spore-producing structures, termed sporangiophores, comprising a stalk (sterigma) and a balloon-like vesicle. The fungal jets eject the spore within 0.01–0.03 ms, launching it at peak accelerations of up to 21,407 g and a maximum velocity of 16 m/s, resulting in a launch distance of 2.5 m at angles ranging from 70° to 90° to the horizontal (52, 64).

This fracture release mechanism is not exclusive to fungi; citrus fruits also exhibit it (65). Oil gland reservoirs in a compressible foam-like layer near the outer surface of citrus fruits rupture under external bending deformation, raising the internal gauge pressure to 0.03–0.14 MPa. This rupture releases high-speed microjets with a diameter of $d_0 = 102 \pm 20 \mu\text{m}$, speeds of $8.5 \pm 4.0 \text{ m/s}$, and accelerations of 5,100 g over distances exceeding 1 mm. The characteristics of these jets are independent of the reservoir or fruit size and lead to the exhaustive ejection of the fruit's aromatic volatile oil. The citrus jets undergo different breakup regimes at $We > 8$ for speeds greater than 1.6 m/s than at $We > 137$, corresponding to speeds over 6.6 m/s (see Section 3 in the **Supplemental Material**). The function of this fluid ejection in citrus fruits remains unknown.

3.2.4. Cobras: precision in venom spitting. *Naja* spp. cobras have evolved a remarkable mechanism for self-defense by spitting venom with high precision. These snakes release fast, pulsed fluid through their microscopic fangs (~500 μm), directing it with high precision toward the eyes of threats up to 2 m away, and they can adjust the distribution of their spit with rapid movements (54, 66, 67) (**Figure 5e**). Spitting cobras exhibit distinct morphological adaptations in their venom delivery system, setting them apart from nonspitting species. A more circular shape of the discharge orifice, for instance, facilitates forward venom ejection, and the venom gland's contraction provides the force needed to propel venom through the hollow fangs. Microscale venom channels, ~5 mm in length and ~500 μm in diameter, feature symmetric ridges along the ventral surface, and a 90° bend near the exit enhances precise control over venom flow (68). Though the venom displays shear-thinning rheology, it shows negligible non-Newtonian effects once in motion, reaching a viscosity of ~44 mPa·s under laminar flow conditions ($Re < 100$). These physical properties ensure a predictable flow of venom. For the cobra *Naja pallida*, the ejection process consists of spits of 0.01 mL over a duration of 40 ms, resulting in average speeds of ~1.27 m/s, with peak exit velocities of 5 to 6 m/s (68).

3.3. Inertio-Gravitational Regime: $Bo > 1$, $We > 1$

Fluid ejection in organisms in which both inertial and gravitational forces dominate the surface tension force constitutes the inertio-gravitational regime ($Bo > 1$, $We > 1$), where ejection is typically in the form of jets and sprays. Within this regime, the Fr (see the sidebar titled Dimensionless

Numbers for Newtonian Liquids in Air) may be relevant to measure the relative effect between inertia and gravity.

Almost all mammals that weigh more than 3 kg urinate in the form of liquid jets and sheets that are within the scope of this regime because of the high hydrostatic pressure due to the length and larger diameter of the urethra. In addition to mammals, other vertebrates such as archerfish and horned lizards use inertio-gravitational jetting for both hunting and defending themselves from predators.

3.3.1. Urination in mammals. Mammals weighing more than 3 kg urinate in liquid jets and sheets in the inertio-gravitational regime due to their large size, where inertia (and gravity) are important and surface tension effects are negligible. The inertio-gravitational regime encompasses urination in a wide range of large mammals with $We \sim \mathcal{O}(10^0-10^2)$ and $Be \sim \mathcal{O}(10^0-10^2)$. The body mass of the animals in this regime ranges from ~ 5 to 5,000 kg, and the size of their bladder varies from 5 mL in cats to 18 L in elephants. The urine flow rate (Q) is proportional to the body mass (M) as $Q \propto M^{0.92}$ within this jetting regime (Figure 5d).

The urination start-up phase is transient, and the jetting dynamics depend largely on the size and shape of the urethra opening and the pressure gradient. In larger animals, urination is driven by higher bladder pressure and hydrostatic pressure (5, 69). Additionally, larger animals also have a longer urethra, resulting in higher hydrostatic pressure, leading to higher flow rates. Thus, larger animals expel larger amounts of liquid with high flow rates in a brief period of time, resulting in an almost constant duration across large mammals (21 ± 13 s), following the law of urination (5) (Figure 5d; Section 3.1.3). In addition, the shape and roughness of the soft and flexible urethra opening vary in different organisms, resulting in the formation of nonaxisymmetric cylindrical jets and irregular urine sheets (5, 70, 71) (Figure 6b,c). The shape factor ($4A/\pi D^2$) of the urethra opening spans 0.14–0.22 for humans to dogs (72), suggesting that the cross-sectional area is $\sim 14\text{--}22\%$ of the equivalent cross-sectional area of the urethra if it is assumed that the urethra is a rigid cylinder.

The urination kinematics of other mammals is largely understudied, and future research should also cover marine mammals such as the blue whale, the largest mammal on Earth. Sei whales and fin whales (*Balaenoptera* spp.) urinate ~ 627 L and ~ 974 L per day (73), respectively, which is 10–20 times the rate of urination in elephants. Further work is needed to address the challenges associated with data collection of marine animals (see Section 4 in the **Supplemental Material**).

3.3.2. Precision hunting in archerfish using water jets. Archerfish (*Toxotes* spp.) actively hunt prey such as flies, spiders, and small lizards in mangrove-filled estuaries and freshwater streams by shooting water jets (Figure 1c). By raising their bony tongue to the roof of their mouth, archerfish form a tube to expel the liquid jet. The speed of the water jet at the opening of the fish mouth is ~ 2 m/s, accelerating to $200\text{--}400$ m/s² and dropping to zero in ~ 15 ms. During the ballistic stage ($\sim 20\text{--}30$ ms), the jet head accelerates and increases in volume. If the tail of the jet is larger than the head, it provides additional thrust, leading to the overall axial compression of the jet. This compression determines the transfer of mass and momentum from the tail to the head of the jet (a phenomenon termed kinematic gathering) (10), resulting in an average impact force of ~ 200 mN, well beyond the anchoring force of small insects and bugs. The jetting in archerfish lies in the inertio-gravitational quadrant of Figure 3, with $We \sim \mathcal{O}(10^2)$ versus $Bo \sim \mathcal{O}(10^0-10^1)$.

Furthermore, a shorter impact time ($\Delta t_i \sim 1\text{--}3$ ms) of the archerfish jets allows momentum transfer. Such a short Δt_i is enabled by kinematic gathering and Rayleigh–Plateau instability, simultaneously amplifying the jet. For a better understanding of jet dynamics, the Rayleigh wavelength is ~ 9 mm and the jet break time (τ_r) is ~ 11 ms for an orifice radius of 1 mm.

Hydrostatic pressure: the pressure exerted by the fluid at equilibrium at any time due to the force of gravity; $P_{\text{hydrostatic}} = \rho g L$, where ρ is the density of urine, g is the acceleration due to gravity, and L is the length of the urethra

Kinematic gathering: in which an accelerating liquid jet exiting the orifice undergoes axial compression, resulting in accumulation of liquid at the front to form a bulky head

Rayleigh wavelength: the distance at which the liquid jet becomes unstable due to Rayleigh–Plateau instability

Supplemental Material >



Figure 6

Jetting phenomena in the inertio-gravitational regime. (a) A horned lizard (*Phrynosoma* sp.) squirts blood from its ocular sinuses. Panel reproduced with permission from J. Dullum/US Fish and Wildlife Service (CC BY 2.0). (b) A goat (*Capra aegagrus hircus*) urinates in the form of a cylindrical jet. Panel adapted with permission from Reference 5. (c) An African bush elephant (*Loxodonta africana*) urinates in the form of a chaotic ejecta sheet. Panel adapted with permission from Reference 5.

As archerfish grow and mature, they refine their jet-shooting skills for hunting, improving the speed and the precision of their jets (74). They even estimate the trajectory of the prey after impact, capturing it before other predators can intervene (75). This ability is particularly impressive when considering factors such as air friction, which can vary with the prey's size and mass. The archerfish's jet amplifies with distance, a phenomenon once thought to be powered by internal structures but is actually due to the kinematic gathering and hydrodynamic instability of the jets, in which the typical specific power of the jet at impact is ~ 300 W/kg—higher than that delivered by a vertebrate muscle (500 W/kg) (76). The archerfish regulates the liquid jet so that the front consists of a single large-volume droplet, delivering a larger momentum to the prey. By modulating the speed of the jet near the mouth, the archerfish increases the mass and speed of the jet front, generating an impact force sufficient to overcome the anchoring force of insects, typically ~ 20 mN (for a body mass of 100 mg) (77).

3.3.3. Defensive blood squirts in horned lizards. Horned lizards (*Phrynosoma* spp.) possess an extraordinary ability to shoot a jet of blood from their ocular sinuses (eye sockets) as a defense mechanism against predators (78, 79). The muscles that line the veins around the eyes of the horned lizard contract, resulting in increased pressure. These lizards expel blood in the form of jets through further abrupt contraction of the muscles. Blood jets or squirts can travel up to a distance of ~ 1 m, aiming to attack predators, generally canids (dogs) (80). The estimated We and Bo for blood squirts in horned lizards are $We \sim \mathcal{O}(10^{-1}-10^1)$ and $Bo \sim \mathcal{O}(10^{-1}-10^1)$. Horned lizards also demonstrate a pattern of repetitive jetting.

3.4. Gravitational Regime: $Bo > 1$, $We < 1$

In this regime, gravitational forces dominate over surface tension and inertial forces. This gravity-driven ejection primarily occurs over extended periods either through micrometer-scale openings (plant guttation) or by slow dripping through millimeter-scale openings (dribbling). Fluid ejection typically occurs as a result of increased forces in fluidic conduits due to high hydrostatic forces or to sudden surges in internal pressure, such as in plant guttation. Owing to small characteristic length scales and insufficient inertia, fluid ejection may lie in a transitional region between the surface tension regime and the gravitational regime. Droplets form at the conduit's tip and grow in size from the steady influx of incoming fluid. When droplets reach a critical mass where gravitational forces overcome surface tension, they detach and fall freely (see the sidebar titled Dripping and Jetting Regimes for Newtonian Fluids). In large nozzles, a low-pressure gradient in the nozzle causes droplet formation and subsequent growth and is followed by free fall under the effect of gravity.

Biologically, the gravitational regime may correspond to residual fluids in a fluidic pipe or to situations where fluid control is less critical. This passive reliance on external gravitational fields can lead to challenges and potential fouling risks. Many biological fluid ejections ultimately transition to this regime, especially at the end of the ejection process, where residual fluid or muscular contraction limitations can cause a dribbling effect (e.g., dribbling after urination).

3.4.1. Plant guttation. Root pressure releases xylem and phloem sap droplets from plant leaves through guttation. Specialized structures termed hydathodes facilitate water exudation at the tip, edges, and margins of leaves (81, 82). Droplets at the leaf apex (or edges) grow in size and fall under gravity or evaporate (**Figure 7a**). Guttation occurs mainly at night when transpiration is absent. Though usually harmless, guttation can promote microbial growth, leading to plant diseases (83). Plant guttation is one of the slowest processes of fluid ejection compared with almost every other example discussed in this review. In the case of *Zantedeschia aethiopica* plants, droplets form and fall in ~ 30 min, with fluid ejection characterized by $We \sim \mathcal{O}(10^{-3})$ and $Bo \sim \mathcal{O}(10^0-10^1)$.

3.4.2. Human tears: basal, reflexive, and emotional tears. Human tears, which are generated by the lacrimal glands, are complex physiological responses to various stimuli. Comprising three layers—an outer oily layer, a central aqueous layer, and an inner mucous layer—tears nourish,

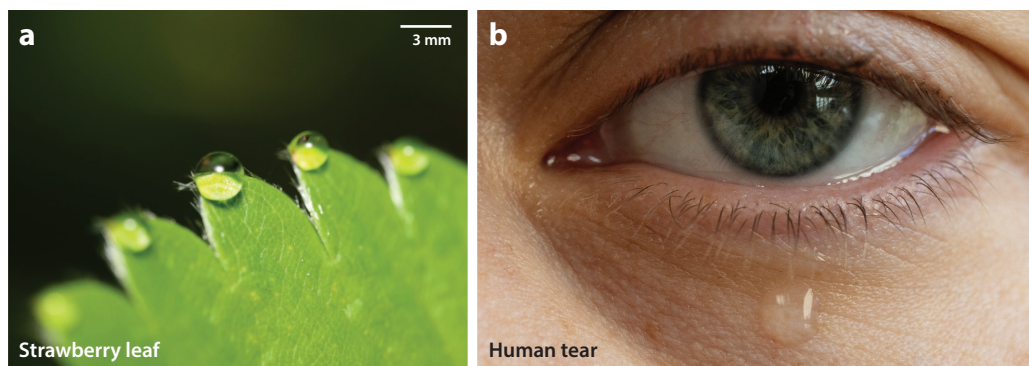


Figure 7

Gravitational fluid ejection in plants and humans. (a) A strawberry plant (*Fragaria* sp.) releases xylem fluid at the leaf tip after a rainy night. The droplets grow until gravitational forces overcome capillary adhesion, leading them to roll off or evaporate. Panel reproduced from Elio J. Challita. (b) Tears flow through openings (puncta) in the eye, and during excessive tearing, tear droplets slowly grow and drain under the influence of gravity.

Non-Newtonian fluids: fluids that exhibit a nonlinear relationship between shear stress and strain rate, with viscosity dependent on the applied shear rate

lubricate, and protect the eyes. Emotional crying involves the brain's limbic system, specifically the hypothalamus, which triggers increased tear production during strong emotions. Emotional tears differ from normal ones, and tears shed by female individuals convey a chemosignal that reduces sexual arousal and testosterone levels in men (84).

Tears flow through puncta openings ($\sim 300\text{--}400\ \mu\text{m}$ in diameter) at the inner corners of the eyelid (**Figure 7b**). Flow rates range from 0.6 to 100 $\mu\text{L}/\text{min}$, depending on the tear type, whether basal, reflexive, or emotional. High flow rates may cause tears to overflow and flow down the cheek, a fluid mechanical phenomenon still understudied.

4. BEYOND THE NEWTONIAN FRAMEWORK: COMPLEX FLUID EJECTIONS IN BIOLOGICAL SYSTEMS

The conventional study of fluid ejections has been largely confined to the Newtonian framework, characterized by Bo and We (**Figure 3**) (see the sidebars titled Dimensionless Numbers for Newtonian Liquids in Air and Dripping and Jetting Regimes for Newtonian Fluids), providing foundational insights into simple fluids with linear shear stress–shear rate relationships. However, biological systems often present more intricate dynamics, including non-Newtonian behaviors that transcend this elementary description (85). In this section, we explore these complex phenomena, extending the discussion to underwater ejections, air–water interfacial dynamics, and complex airborne fluids. We delve into fluid–fluid interfacial dynamics, including Marangoni effects at the air–water interface, which were beyond the scope of the focus on aerial fluid ejection in Section 3. We also explore the complexity of multiphase flows, such as atomization, aerosolization, and turbulence, extending beyond the single-phase liquid ejection within the Newtonian framework. We discuss the unique shapes and properties of biological nozzles, including elastic, corrugated, and soft types, which introduce elastocapillarity and elastohydrodynamic instabilities to the ejected fluid. These complexities provide a more comprehensive understanding of jets and sprays, reflecting the multifaceted nature of fluid ejections in biological systems, and set the stage for a detailed examination of complex fluids in the subsequent sections.

4.1. Non-Newtonian Fluid Ejections in Living Systems: A Rheological Perspective

Non-Newtonian fluids, characterized by nonlinear relationships between shear stress and strain rate, offer a broader perspective that encompasses the complex behaviors found in nature. These fluids, whose viscosity depends on the applied shear rate, are employed by organisms for various functions such as locomotion, protection, hunting, and reproduction.

Most non-Newtonian fluids in nature are viscoelastic, possessing both viscous and elastic components. Unlike Newtonian fluids, viscoelastic fluids resist extension, leading to unique phenomena such as beads on a string (86, 87). These complex behaviors are characterized by dimensionless numbers such as Deborah (De) and Weissenberg (Wi) numbers [defined in the sidebar titled Dimensionless Numbers for Non-Newtonian (Viscoelastic) Fluids] and are essential for understanding viscoelastic flow (88, 89).

Viscoelastic fluids are ubiquitous in nature and industry, found in organisms such as pitcher plants, deep-sea hagfish, velvet worms, and termites, as well as in industrial applications such as food production, blood testing, adhesives, and paints (59, 90–93). The transition to a more complex understanding of fluid ejections, beyond the Newtonian framework described in Section 3, holds significant relevance for real-world applications, potentially uncovering new avenues in fields such as additive manufacturing and drug delivery. The exploration of these complex phenomena underscores the need for further research and the challenges in characterizing these intricate fluid behaviors.

DIMENSIONLESS NUMBERS FOR NON-NEWTONIAN (VISCOELASTIC) FLUIDS

The following dimensionless numbers are essential for characterizing the ejection of non-Newtonian fluids:

$$\text{Deborah number, } De = \frac{\lambda}{T}, \quad \text{and} \quad \text{Weissenberg number, } Wi = \frac{\lambda v}{L}.$$

Essentially, De is the ratio of the characteristic time of the fluid (λ) to the observation time (T), and it determines the degree to which elasticity is expressed in response to a transient deformation. Wi is the product of the characteristic time of the fluid and the characteristic rate of deformation (v/L , where v is the fluid velocity at the nozzle exit and L is the characteristic length of the nozzle).

These numbers are particularly useful for characterizing viscoelastic flows, representing the ratio of elastic to viscous forces, and correlating the fluid's relaxation time with the observation time (88, 89). Their application in fluid ejection in living systems has been limited, but they hold the potential to gain insights into the rheological behavior of non-Newtonian fluids in nature and the industrial and natural contexts related to them.

4.1.1. Active nozzle control in velvet worms' slime jets. Velvet worms (phylum Onychophora) eject slime jets, an extraordinary example of organismal fluid ejection, by leveraging actively controlled soft nozzles (92, 94). **Figure 8a** shows an example of slime jetting in velvet worms. Several species of velvet worms can be found in Southeast Asia, Central America, and South America. Slime jets display an elastohydrodynamic instability, resulting in oscillatory motion. Velvet worms slowly contract their slime reservoir, forcing the slime through a narrow duct, and control this contraction to enhance jet speed. The ejected jets reach speeds of ~ 3 to 5 m/s over a duration of ~ 64 ms and oscillate at frequencies of ~ 30 – 60 Hz (92). Employed for both defensive and predatory purposes, slime forms a web-like pattern that hardens to trap and capture prey.

4.1.2. Spitting spiders: oscillatory viscoelastic threads. Spitting spiders (*Scytodes* spp.) utilize a complex mechanism to discharge a combination of silk, venom and adhesive through their fangs, creating a distinctive zigzag pattern (93, 96, 98) (**Figure 8b**). This pattern is formed due to the oscillatory motion of the fangs, with the spit exiting through a narrow orifice ~ 14 μm in diameter. The ejection lasts 35 ms and reaches a maximum speed of 28 m/s, with oscillating frequency reaching up to ~ 2 kHz and averaging ~ 1 kHz.

The zigzag pattern results from the fangs' oscillation along the lateral–medial axis coupled with a traversing motion from ventral to dorsal due to the elevation of the chelicerae (96). This motion leads to the production of glue beads on silk threads during lateral-to-medial sweeps of the fangs, while medial-to-lateral sweeps produce simple fibers. This behavior, reminiscent of the beads-on-a-string phenomenon, requires further investigation, particularly as viscoelastic jetting from narrow elastic nozzles of $\mathcal{O}(10^1)$ μm holds special interest for industrial applications.

The high oscillation frequencies observed in this process are likely caused by hydrodynamic forcing, generated as the fluid is ejected through the narrow elastic nozzle. Additionally, asynchronous coupling with muscles may contribute to this phenomenon, where a single muscle contraction can induce an oscillatory motion of the fangs (96). This intricate mechanism demonstrates the complexity of fluid dynamics in biological systems and underscores the need for detailed study and characterization.

4.1.3. Adhesive locomotion: gastropods' viscoelastic mucus. Gastropods (snails and slugs) utilize viscoelastic mucus for adhesive locomotion (85, 99). **Figure 8c** shows a slime trail left by a

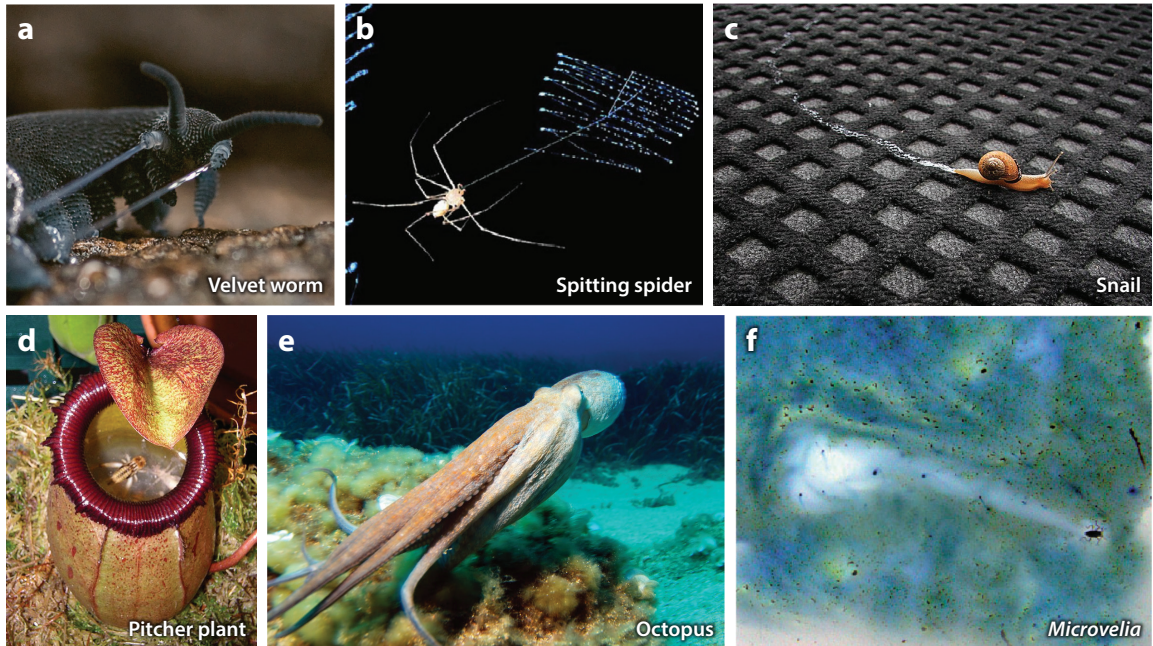


Figure 8

Examples of complex fluid ejections in nature. (a) A velvet worm (*Euperipatoides rowelli*) shoots viscoelastic jets for defense. Panel reproduced from Reference 95. (b) A spitting spider (*Scytodes thoracica*) spits viscoelastic jets in a zigzag formation. Panel reproduced from Reference 96. (c) A snail (Gastropoda) leaves a slime trail, which is exuded under its muscular foot for adhesive locomotion. Panel reproduced with permission from Trina Yount. (d) A pitcher plant (*Nepenthes sibuyanensis*) traps a fly in its viscoelastic fluid. (e) A common octopus (*Octopus vulgaris*) employs jet propulsion to locomote underwater in the Mediterranean Sea. Panel reproduced from Getty Images. (f) *Microvelia* moves across the water surface using Marangoni propulsion by ejecting surface-active fluids through its proboscis, leaving a white trail by displacing the dye. Panel reproduced from Reference 97.

snail. Consisting mostly of water, with glycoproteins accounting for less than 10%, the mucus is viscoelastic and forms a thin layer of $\sim 10\text{--}20 \mu\text{m}$ (100). To move on this mucus film, gastropods create muscular waves along their ventral side, which are composed of alternating contractions and relaxations (101, 102). During contraction, these waves are transmitted to the mucus layer, which undergoes large strains that disrupt the mucus network. This elastic solid-like material yields at large strain rates and behaves like a viscous fluid. During the relaxation stage, the mucus heals and reforms its gel network, allowing locomotion (100). The rhythmic discharge of mucus is controlled by the fluctuating blood pressure in the gastropod's foot through pores in the epidermis (103).

4.1.4. Defensive slime ejection: hagfish's rapid response. Hagfish (Myxinidae), which are eel-shaped marine fish, can generate a large amount of slime in a very short period of time, releasing it from their ventral pores into the ocean (91, 104). Hagfish dwell in the deep ocean and feed near the seafloor. The slime ejected by hagfish comes in contact with water and undergoes physicochemical reactions to form a fibrous gel with ultralong threads of protein and hydrated mucus, rendering it flexible for an effective defense mechanism. When provoked, hagfish eject slime, blocking the mouth and gills of their predators (105, 106), helping them escape. Rheologically, the slime exhibits elongational thickening during predator suction feeding and shear thinning during

Marangoni propulsion: a net propulsion due to an interfacial flow generated in the direction of increasing surface tension using surface-active fluids

their escape. Furthermore, hagfish slime is expected to behave as a drag-reducing agent. Some studies limited to low concentrations showed negligible drag reduction through evaluation of Wi , and future studies using higher concentrations are required in order to characterize this behavior (107).

4.1.5. Carnivorous plants: predatory capture with viscoelasticity. Carnivorous pitcher plants of the genus *Nepenthes* secrete viscoelastic fluids to capture prey (108). **Figure 8d** presents insects trapped in a pitcher plant's fluid. In *Nepenthes rafflesiana*, the capture rate of flies and ants is higher (nearly 100%) when De is greater than unity (i.e., $De > 1$). This indicates that higher capture rates occur when the fluid's elastic forces do not have time to relax due to the insect's swimming strokes. De is the ratio of the elastic relaxation time of the fluid to the half-period of the swimming stroke of the insect. For $De \leq 0.1$, the capture rate of the flies is as low as 0%, while the capture rate of the ants is $\sim 20\%$. The lower surface tension of the fluid (~ 60 mN/m) also aids in sinking the prey (109).

4.2. Fluid-Driven Propulsion: Navigating Underwater and Air-Water Interfaces

Aquatic and semiaquatic organisms often achieve rapid propulsion underwater or at the air-water interface by either ejecting fluid from their bodies or utilizing environmental fluid. This section explores various mechanisms and examples of fluid ejection for propulsion.

4.2.1. Underwater jet propulsion in aquatic invertebrates. Marine invertebrates such as cephalopods (octopuses, squids, and cuttlefish), jellyfish, and insect larvae employ jet propulsion for high-speed locomotion underwater (2, 14, 110–112). Pulsed jetting, the pressure created by the pulse jetting behind the organism, produces almost 30% more thrust than a continuous jet (113). Squids, chordates, octopus, and jellyfish utilize this mechanism. **Figure 8e** shows an octopus locomoting via jet propulsion under water. Squids, for example, are among the fastest marine invertebrates, achieving maximum speeds of 5 to 10 m/s through pulsatile jet propulsion (114). To achieve this, squids use their body cavity as a pressure chamber and a narrow tube termed a siphon for the expulsion of water (114, 115). The elasticity of the cavity wall and specific muscles power body deformation, enabling pulsatile jetting for burst propulsion (115, 116). Salps, a type of chordate, create pulse jets with speeds of ~ 3.3 cm/s ($Re \sim 200$ –400) and usually swim at a rate of 1.2 to 1.7 cm/s (14, 117). Jellyfish also use single jets for locomotion and predator evasion (14).

Dragonfly larvae utilize their hindguts as extreme biological pumps, ejecting repetitive jets from their anus for propulsion underwater. They modulate the orifice of the anus using an anal valve with a reported diameter of 0.4 mm. The velocity of the jet during propulsion typically ranges from 1 to 2 m/s, with each jet lasting 100 ms, resulting in an estimated swimming speed of 10 cm/s (118, 119).

4.2.2. Harnessing surface tension: Marangoni propulsion in water striders. Water striders from the genera *Microvelia* and *Velia* (family Veliidae), along with rove beetles of the genus *Stenus* (family Staphylinidae), have developed a remarkable method of rapid escape from predators by utilizing Marangoni propulsion at the air-water interface (120–122). **Figure 8f** shows *Microvelia* locomoting on water using Marangoni propulsion. These insects eject surface-active fluids that lower the surface tension behind them, propelling them forward. *Stenus* rove beetles employ this mechanism to achieve speeds up to 45–70 cm/s, nearly 30 times faster than their normal swimming speeds (120). Similarly, *Microvelia* species use their proboscis to eject surfactants, reaching speeds up to 17 cm/s, slightly exceeding their water-running speed (97, 123).

4.3. Explosive Expulsions: Unleashing Multiphase Sprays

The explosive expulsion of fluids, whether through human sneezes or dolphin blowholes, showcases the intricate interplay between biomechanics and fluid dynamics. These multiphase sprays not only provide insight into biological functions but also open doors for applications in fields like medical diagnostics and marine biology. The following sections explore specific examples, shedding light on the underlying mechanisms and potential applications.

4.3.1. Human sneezes: turbulent clouds of aerosols. When humans sneeze or cough, they release turbulent clouds of aerosols and droplets from the nose and mouth (124, 125). This process begins with the buildup of air pressure in the lungs, which, upon sudden opening of the glottis, bursts forth as a multiphase flow. The maximum speed of this flow during a sneeze reaches ~ 15 m/s (126). These droplets often contain pathogens, leading to the transmission of respiratory diseases when spread through coughing or sneezing (127).

4.3.2. Chuffing in dolphins and whales: characterizing blowhole ejections. Dolphins and whales eject turbulent two-phase impulsive jets composed of air, mucus, and water, a phenomenon known as chuffing. Before taking a new breath, they forcefully expel these multiphase contents from their lungs (128, 129). The whale blowholes, ~ 50 cm in size, allow for ejections that last ~ 0.3 s and reach maximum speeds of up to ~ 27.5 m/s (130). Marine scientists are particularly interested in collecting mucus from these ejections, despite the challenges, as it helps gauge the stress levels of these marine mammals (**Figure 1f**).

4.4. Insect Arsenal: Chemical Warfare and Fluid Dynamics

Insects exhibit remarkable abilities in ejecting chemical sprays for defense, showcasing a complex interplay between chemistry and fluid dynamics (56, 58). Bombardier beetles, European wood ants, and twostriped walkingsticks (*Anisomorpha buprestoides*) employ these chemical tactics (131, 132).

Bombardier beetles store a reactant solution (hydrogen peroxide, hydroquinones, and alkanes) and a solution of peroxidase and catalase enzymes in separate chambers. During ejection, these chemicals interact, facilitating an exothermic reaction that forms a mixture of quinones, ejected at a scalding 100°C . The beetles discharge this defensive spray as a pulsating jet at a rate of 500 pulses per second, with a typical speed of ~ 10 m/s and a duration of ~ 11 ms (132, 133).

The twostriped walkingstick, on the other hand, fends off predators by ejecting a milky white fluid up to 30–40 cm away (134). Secreted from glands near the thorax and containing terpene dialdehyde (135), this fluid effectively deters various organisms, including ants, beetles, and birds.

The fluid dynamics associated with these ejections is equally fascinating. For example, the bombardier beetle controls the direction of the spray discharge using the Coanda (136), a phenomenon where the fluid flows along the curvature of a surface. The study of chemical warfare and fluid ejections in insects, particularly in unsteady and complex environments, remains an open and intriguing area of research, offering promising avenues for understanding biological functions and potential applications in various fields.

4.5. Intricate Characteristics of Nature's Fluidic Conduits

The study of fluid ejection in nature extends beyond simple geometries, delving into the complex and multifaceted world of biological conduits. The following sections explore the elasticity, corrugations, and geometry of these conduits, shedding light on the intricate dynamics that govern fluid flow in living organisms.

4.5.1. Elasticity: interplay of form and function. Elasticity within a nozzle significantly influences jetting dynamics. Pressure-driven flow through an elastic pipe may lead to pipe expansion, altering its shape and configuration and potentially giving rise to instabilities. This phenomenon is observed in the mammalian urethral lumen, which can enlarge during peristaltic action (137). Velvet worms exemplify this, employing a syringe-like ejection mechanism with a flexible, accordion-shaped oral papilla to emit a slime-like jet. The resulting fluid ejection exhibits large, rapid oscillations, enabling the coating of extensive prey surfaces. These oscillations stem from the interplay between fluid inertia and papilla elasticity, allowing high-frequency jet oscillations without the need for rapid muscle contractions or neural control (138).

4.5.2. Corrugations: hidden complexities. Biological conduits often feature nonsmooth interiors with surface structures, adding complexity to fluid flow. The mammalian urethra's corrugations, for example, reduce the effective pipe area and flow speed (70, 137). This internal roughness becomes pronounced under high-Reynolds-number conditions ($Re > 2,300$), where inertia plays a significant role. The interaction of the fluid with these internal structures affects the shape and breakup of the exiting jet, adding layers of complexity to the flow profile (139) (see Section 4 in the **Supplemental Material**).

4.5.3. Geometry: shaping the flow. The noncircular geometries of biological pipes and nozzles, including elliptical, triangular, rectangular, and tapered shapes, influence the fluid flow profile within a channel and the hydrostatic resistance. These geometrical effects may be accounted for using a correction factor α (140). Nozzle shape may also affect droplet size during dripping, with circular nozzles yielding the largest droplets at a given critical pressure. For example, droplet volume reduced by 18% with a triangular nozzle with stretched corners compared with a circular one. Such noncircular nozzles enable more tailored fluid control by leveraging geometry, which may be the case in certain biological systems (141).

5. HARNESSING FLUID EJECTIONS IN LIVING SYSTEMS: A PATHWAY TO INNOVATION

Nature's organisms have evolved sophisticated mechanisms for fluid ejection to carry out essential activities such as hunting, eating, self-defense, and excretion. Beyond the scientific curiosity to unravel these fascinating processes, there is a wealth of knowledge to be gleaned for technical applications. Drawing inspiration from natural systems has already led to innovations such as insect flight-inspired aerial vehicle designs (142), gecko-inspired adhesive materials (143), and superhydrophobic structures inspired from lotus leaves (144). Similarly, fluid ejection systems in living organisms present a range of potential technological applications.

Sharpshooters launch their urine droplets using superpropulsion, an energy-efficient method of expelling liquid droplets (34). This mechanism could be applied to water removal from electronic gadgets, such as smartwatches, which rely on vibration-induced water removal (**Figure 9a**). Combined with existing methods that use an acoustic signal, superpropulsion could enhance the effectiveness of water expulsion (145).

The pulsed jetting mechanisms in archerfish have potential applications in inkjet printing and drug delivery (**Figure 9b**). Archerfish use an active nozzle to increase the momentum of the jet's front, a technique that could be applied to jet injections of medications beneath the skin (147). The repetitive and continuous drop formation in archerfish jets could also be harnessed for inkjet printing.

Organisms such as velvet worms, spitting spiders, and termites shoot jets of viscoelastic material through small openings (92, 96) (**Figure 9c**). In additive manufacturing, ejecting viscoelastic fluid

Supplemental Material >

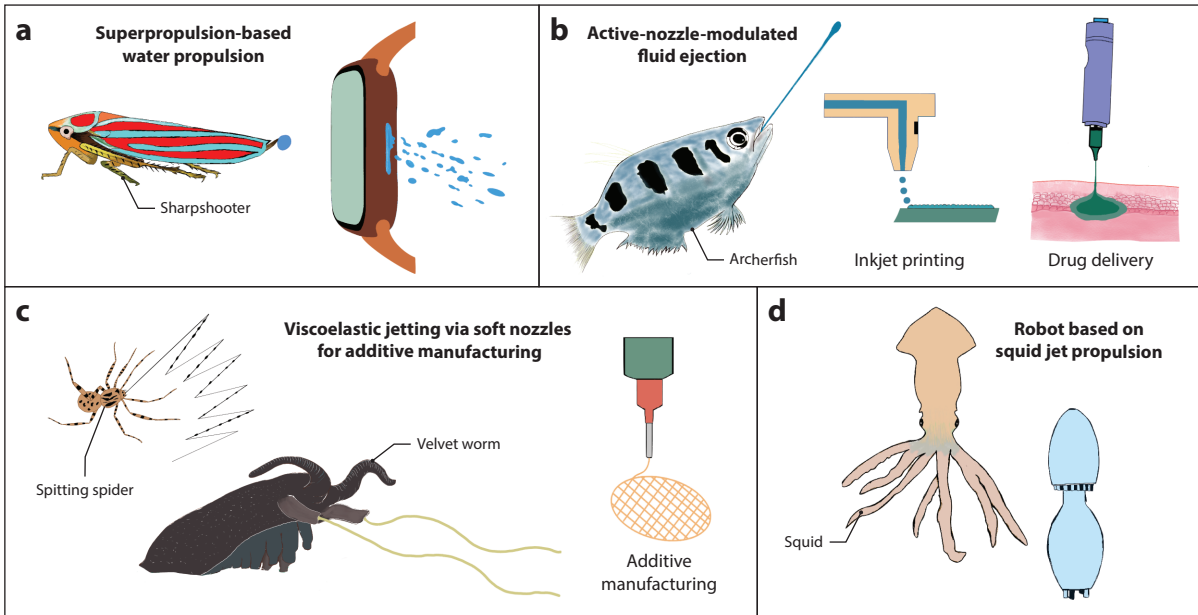


Figure 9

Innovative applications inspired by natural fluid ejections. (a) Expulsion of water from electronic gadgets like smartwatches, utilizing the superpropulsion phenomenon observed in sharpshooters (4). (b) The jetting phenomenon in archerfish, applicable in drug delivery and inkjet printing (77). (c) Micron-scale viscoelastic jetting via soft nozzles in velvet worms and spitting spiders, offering insights for nozzle design in additive manufacturing. (d) Squid-inspired robots employing jet propulsion for rapid and efficient locomotion (146).

through narrow micrometer-scale orifices has been challenging. Studying the nozzle structure of these organisms could guide the design of flexible and robust nozzles for applications such as 3D printing of hydrogels.

The study of ejection mechanisms and fluid dynamics in underwater organisms such as jellyfish, octopuses, squids, and dragonfly larvae has inspired the development of efficient underwater robots (148–150). These natural propulsion systems offer valuable insights for creating innovative and effective robotic designs (Figure 9d).

Other interesting applications include the development of the μ Mist system by Swedish Biomimetics, which is based on flash evaporation of the liquid while exiting a chamber to form a spray and is inspired by the spray formation mechanism in bombardier beetles (151). Furthermore, the coalescence-inducing drop jumping mechanism observed in fungal spores can be used in various applications, such as self-cleaning of surfaces, heat transfer, and anti-icing (30, 46).

6. CONCLUDING REMARKS

In this review, we have dissected fluid ejections in biological systems across scales, unraveling underlying physical principles and biological functions. The intersection of biomechanics and fluid dynamics has provided insights into how organisms handle fluids, from repetitive ejections for functions like excretion and hunting to single-shot, destructive ejections in fungi and insects.

We have identified diverse mechanisms, including muscle contraction, gravity, and surface tension, leading to a wide spectrum of fluid ejections. Large living systems rely on gravity and inertia, while small living systems depend on surface tension and inertia, with complex dynamics in both.

Beyond the Newtonian framework, we have explored intricate fluid dynamics of complex fluids, opening new avenues for technological innovation. The control over ejected fluid has been a focal point, emphasizing the balance organisms must achieve for specific functional needs.

Open areas for research abound, from the excretion dynamics of cicadas to the chuffing of marine animals such as whales. Investigating these unexplored territories may reveal insights into broader ecological patterns and environmental responses. These phenomena may serve as non-invasive biofluid diagnostics, offering insights into ecosystem health and the effects of climate change, akin to how human sneezing helps us to understand disease transmission.

The use of active nozzles by organisms such as conehead termites, spitting spiders, velvet worms, and archerfish to control complex fluid ejection remains an understudied area. It holds immense potential in designing smart nozzles for applications ranging from drug delivery to on-demand printing in food engineering to additive manufacturing.

Although beyond the scope of this review, this topic is ripe for discovery. From the unexplored realms of cellular ejection in bacteria and protozoa to diatoms' adhesive ejection for locomotion, this review serves as a springboard to nature's immense fluid ejections waiting to be discovered. As we find the marvelous in the mundane, these phenomena continue to open a world of exploration and inspiration.

SUMMARY POINTS

1. Nature's fluid ejections are diverse, spanning various taxa, timescales, and physical scales.
2. We present a framework for dripping and jetting based on the Bond (Bo) and Weber (We) numbers, dividing fluid ejections into four quadrants: surface tension regime ($Bo < 1, We < 1$), inertio-capillary regime ($Bo < 1, We > 1$), inertio-gravitational regime ($Bo > 1, We > 1$), and gravitational regime ($Bo > 1, We < 1$).
3. In the surface tension regime ($Bo < 1, We < 1$), organisms overcome fluid adhesion challenges by exploiting surface tension properties, such as ejecting droplets using elasticity, reducing it with coatings, or relying on external agents. Some organisms even leverage capillary adhesion for evaporative cooling, akin to mammalian sweating.
4. In the inertio-capillary regime ($Bo < 1, We > 1$), inertial forces dominate, with surface tension more significant than gravity. Here, small organisms must overcome surface tension and viscous forces to pump fluids at high speeds. This regime includes diverse mechanisms such as fracture-based ejections (fungal cannon and citrus glands) and defensive strategies (wood ants and *Nasutitermes* termites), as well as jet urination in large insects.
5. In the inertio-gravitational regime ($Bo > 1, We > 1$), inertia and gravity drive fluid ejection as liquid jets and sheets. Examples include urination in large animals and the shooting of jets by archerfish and horned lizards for predation and defense.
6. The gravitational regime ($Bo > 1, We < 1$) involves gravity-driven fluid flow from nozzles, either as very slow dripping from small nozzles or as immediate flow from large ones. Most quadrants converge into this regime at the end of their fluid ejections.
7. A significant subset of fluid ejection in nature falls outside the Newtonian framework of We versus Bo . The complex dynamics of phenomena such as slime ejection in terrestrial and marine organisms and Marangoni propulsion in *Microvelia* demand further study.

8. The applications of fluid ejections in nature, from electronic gadgets to underwater propulsion of robots, are endless and warrant diligent exploration.

DISCLOSURE STATEMENT

The authors are not aware of any affiliations, memberships, funding, or financial holdings that might be perceived as affecting the objectivity of this review.

ACKNOWLEDGMENTS

The authors thank Sheila Patek, Sunny Jung, David Hu, and Simon Sponberg for their valuable help and suggestions, and Prateek Sehgal and Jaime Quispe Nina for their help in data collection and analysis of the cicada data in Peru. They also thank the Bhamla lab for helpful discussions and comments. M.S.B. acknowledges funding support from National Institutes of Health grant R35GM142588; National Science Foundation grants POLS-2310691, CAREER IOS-1941933, MCB-1817334, CMMI-2218382, and EF-1935262; and the Open Philanthropy Project. P.R. acknowledges the financial support provided by the Eckert Postdoctoral Fellowship from the Georgia Institute of Technology.

LITERATURE CITED

1. Pfister L, Savenije HH, Fenicia F. 2009. *Leonardo da Vinci's Water Theory: On the Origin and Fate of Water*. Oxfordshire, UK: IAHS Press
2. Vogel S. 1996. *Life in Moving Fluids: The Physical Biology of Flow*. Princeton, NJ: Princeton Univ. Press. 2nd ed.
3. Marusic I, Broomhall S. 2021. Leonardo da Vinci and fluid mechanics. *Annu. Rev. Fluid Mech.* 53:1–25
4. Challita EJ, Sehgal P, Krugner R, Bhamla MS. 2023. Droplet superpropulsion in an energetically constrained insect. *Nat. Commun.* 14:860
5. Yang PJ, Pham J, Choo J, Hu DL. 2014. Duration of urination does not change with body size. *PNAS* 111:11932–37
6. Weiss MR. 2006. Defecation behavior and ecology of insects. *Annu. Rev. Entomol.* 51:635–61
7. Eisner T, Aneshansley DJ. 1999. Spray aiming in the bombardier beetle: photographic evidence. *PNAS* 96:9705–9
8. Keller B, Willke T. 2019. Snotbot: a whale of a deep-learning project. *IEEE Spectr.* 56:41–53
9. Richter JP, ed. 2012. *The Notebooks of Leonardo da Vinci*, Vol. 1. North Chelmsford, MA: Courier Corp.
10. Eggers J, Villermaux E. 2008. Physics of liquid jets. *Rep. Prog. Phys.* 71:036601
11. van Hoeve W, Gekle S, Snoeijer JH, Versluis M, Brenner MP, Lohse D. 2010. Breakup of diminutive Rayleigh jets. *Phys. Fluids* 22:122003
12. Clanet C, Lasheras JC. 1999. Transition from dripping to jetting. *J. Fluid Mech.* 383:307–26
13. Fuller GG, Vermant J. 2012. Complex fluid-fluid interfaces: rheology and structure. *Annu. Rev. Chem. Biomol. Eng.* 3:519–43
14. Gemmell BJ, Dabiri JO, Colin SP, Costello JH, Townsend JP, Sutherland KR. 2021. Cool your jets: biological jet propulsion in marine invertebrates. *J. Exp. Biol.* 224:jeb222083
15. de Gennes PG, Brochard-Wyart F, Quéré D. 2004. *Capillarity and Wetting Phenomena: Drops, Bubbles, Pearls, Waves*. New York: Springer
16. Bush J. 2010. Interfacial phenomena. Course 18.357, Fall. Mass. Inst. Technol., Cambridge
17. Lin SP, Reitz RD. 1998. Drop and spray formation from a liquid jet. *Annu. Rev. Fluid Mech.* 30:85–105
18. Bergman EA, Green EL, Matthews PGD. 2021. The cibarial pump of the xylem-feeding froghopper (*Philaenus spumarius*) produces negative pressures exceeding 1 MPa. *Proc. R. Soc. B* 288:20210731
19. Clanet C, Lasheras JC. 1999. Transition from dripping to jetting. *J. Fluid Mech.* 383:307–26

20. Denny M. 1993. *Air and Water: The Biology and Physics of Life's Media*. Princeton, NJ: Princeton Univ. Press
21. Hu DL, Bush JW. 2005. Meniscus-climbing insects. *Nature* 437:733–36
22. Ortega-Jimenez VM, Challita EJ, Kim B, Ko H, Gwon M, et al. 2022. Directional takeoff, aerial righting, and adhesion landing of semiaquatic springtails. *PNAS* 119:e2211283119
23. Liu F, Chavez RL, Patek SN, Pringle A, Feng JJ, Chen CH. 2017. Asymmetric drop coalescence launches fungal ballistospores with directionality. *J. R. Soc. Interface* 14:20170083
24. Pike N, Richard D, Foster W, Mahadevan L. 2002. How aphids lose their marbles. *Proc. R. Soc. B* 269:1211–15
25. Folk GE, Semken A. 1991. The evolution of sweat glands. *Int. J. Biometeorol.* 35:180–86
26. Kasahara M, Akimoto S-i, Hariyama T, Takaku Y, Yusa S-i, et al. 2019. Liquid marbles in nature: craft of aphids for survival. *Langmuir* 35:6169–78
27. Lahondère C, Lazzari CR. 2012. Mosquitoes cool down during blood feeding to avoid overheating. *Curr. Biol.* 22:40–45
28. Stolze-Rybczynski JL, Cui Y, Stevens MHH, Davis DJ, Fischer MW, Money NP. 2009. Adaptation of the spore discharge mechanism in the Basidiomycota. *PLOS ONE* 4:e4163
29. Buller AHR. 1922. *Researches on Fungi*, Vol. 2. London: Longmans, Green & Co.
30. Liu C, Zhao M, Zheng Y, Cheng L, Zhang J, Tee CAT. 2021. Coalescence-induced droplet jumping. *Langmuir* 37:983–1000
31. Redak RA, Purcell AH, Lopes JR, Blua MJ, Mizell RF III, Andersen PC. 2004. The biology of xylem fluid-feeding insect vectors of *Xylella fastidiosa* and their relation to disease epidemiology. *Annu. Rev. Entomol.* 49:243–70
32. Okumura K, Chevy F, Richard D, Quéré D, Clanet C. 2003. Water spring: a model for bouncing drops. *Europhys. Lett.* 62:237–43
33. Hubert M, Robert D, Caps H, Dorbolo S, Vandewalle N. 2015. Resonant and antiresonant bouncing droplets. *Phys. Rev. E* 91:023017
34. Raufaste C, Chagas GR, Darmanin T, Claudet C, Guittard F, Celestini F. 2017. Superpropulsion of droplets and soft elastic solids. *Phys. Rev. Lett.* 119:108001
35. Szczepanski CR, Guittard F, Darmanin T. 2017. Recent advances in the study and design of parahydrophobic surfaces: from natural examples to synthetic approaches. *Adv. Colloid Interface Sci.* 241:37–61
36. Andersen PC, Brodbeck BV, Mizell RF III 1989. Metabolism of amino acids, organic acids and sugars extracted from the xylem fluid of four host plants by adult *Homalodisca coagulata*. *Entomol. Exp. Appl.* 50:149–59
37. Novotny V, Wilson MR. 1997. Why are there no small species among xylem-sucking insects? *Evol. Ecol.* 11:419–37
38. Berlin LC, Hibbs ET. 1963. Digestive system morphology and salivary enzymes of the potato leafhopper, *Empoasca fabae* (Harris). *Proc. Iowa Acad. Sci.* 70:527–40
39. Wang W, Ji C, Lin F, Zou J, Dorbolo S. 2019. Water drops bouncing off vertically vibrating textured surfaces. *J. Fluid Mech.* 876:1041–51
40. Fokkema N, Riphagen I, Poot R, De Jong C. 1983. Aphid honeydew, a potential stimulant of *Cochliobolus sativus* and *Septoria nodorum* and the competitive role of saprophytic mycoflora. *Trans. Br. Mycol. Soc.* 81:355–63
41. Benton T, Foster W. 1992. Altruistic housekeeping in a social aphid. *Proc. R. Soc. B* 247:199–202
42. Mahadevan L. 2001. Non-stick water. *Nature* 411:895–96
43. Broadbent L. 1951. Aphid excretion. *Proc. R. Entomol. Soc. A Gen. Entomol.* 26:97–103
44. Harner AD, Leach HL, Briggs L, Centinari M. 2022. Prolonged phloem feeding by the spotted lanternfly, an invasive planthopper, alters resource allocation and inhibits gas exchange in grapevines. *Plant Direct* 6:e452
45. Pringle A, Patek SN, Fischer M, Stolze J, Money NP. 2005. The captured launch of a ballistospore. *Mycologia* 97:866–71
46. Mouterde T, Nguyen TV, Takahashi H, Clanet C, Shimoyama I, Quéré D. 2017. How merging droplets jump off a superhydrophobic surface: measurements and model. *Phys. Rev. Fluids* 2:112001

47. Heinrich B. 1979. Keeping a cool head: honeybee thermoregulation. *Science* 205:1269–71
48. Heinrich B. 1976. Heat exchange in relation to blood flow between thorax and abdomen in bumblebees. *J. Exp. Biol.* 64:561–85
49. Adams PA, Heath JE. 1964. An evaporative cooling mechanism in *Pholus achemon* (Sphingidae). *J. Res. Lepidopt.* 3:69–72
50. Prange HD. 1996. Evaporative cooling in insects. *J. Insect Physiol.* 42:493–99
51. McKinley GH, Renardy M. 2011. Wolfgang von Ohnesorge. *Phys. Fluids* 23:127101
52. Yafetto L, Carroll L, Cui Y, Davis DJ, Fischer MW, et al. 2008. The fastest flights in nature: high-speed spore discharge mechanisms among fungi. *PLOS ONE* 3:e3237
53. Brütsch T, Jaffuel G, Vallat A, Turlings TC, Chapuisat M. 2017. Wood ants produce a potent antimicrobial agent by applying formic acid on tree-collected resin. *Ecol. Evol.* 7:2249–54
54. Young BA, Dunlap K, Koenig K, Singer M. 2004. The buccal buckle: the functional morphology of venom spitting in cobras. *J. Exp. Biol.* 207:3483–94
55. McGavin GC, Davranoglou LR, Lewington R. 2023. *Essential Entomology*. Oxford, UK: Oxford Univ. Press
56. Eisner T, Eisner M, Siegler M. 2005. *Secret Weapons: Defenses of Insects, Spiders, Scorpions, and Other Many-Legged Creatures*. Cambridge, MA: Harvard Univ. Press
57. Eisner T, Kriston I, Aneshansley DJ. 1976. Defensive behavior of a termite (*Nasutitermes exitiosus*). *Behav. Ecol. Sociobiol.* 1:83–125
58. Blum MS. 2012. *Chemical Defenses of Arthropods*. New York: Elsevier
59. Challita E, Rohilla P, Schgal P, Harrison J, Bhamla S. 2023. The dynamics of microjet spitting in termite soldiers. Abstract presented at the American Physical Society March Meeting 2023, Las Vegas, NV, Mar. 5–10
60. Challita EJ, Bhamla MS. 2024. Unifying fluidic excretion across life from cicadas to elephants. *PNAS* 121(13):e2317878121
61. Sakes A, van der Wiel M, Henselmans PW, van Leeuwen JL, Dodou D, Breedveld P. 2016. Shooting mechanisms in nature: a systematic review. *PLOS ONE* 11:e0158277
62. Kohlmeyer J, Volkmann-Kohlmeyer B. 1996. Fungi on *Juncus roemerianus*. 6. *Glomerobolus* gen. nov., the first ballistic member of Agonomycetales. *Mycologia* 88:328–37
63. Van Leeuwen JL. 2010. Launched at 36,000g. *Science* 329:395–96
64. Money NP, Fischer MW. 2009. Biomechanics of spore release in phytopathogens. In *Plant Relationships: The Mycota*, ed. HB Deising, pp. 115–33. Berlin: Springer
65. Smith NM, Ebrahimi H, Ghosh R, Dickerson AK. 2018. High-speed microjets issue from bursting oil gland reservoirs of citrus fruit. *PNAS* 115:E5887–95
66. Westhoff G, Tzschätzsch K, Bleckmann H. 2005. The spitting behavior of two species of spitting cobras. *J. Comp. Physiol. A* 191:873–81
67. Berthé RA, De Pury S, Bleckmann H, Westhoff G. 2009. Spitting cobras adjust their venom distribution to target distance. *J. Comp. Physiol. A* 195:753–57
68. Triep M, Hess D, Chaves H, Brücker C, Balmert A, et al. 2013. 3D flow in the venom channel of a spitting cobra: Do the ridges in the fangs act as fluid guide vanes? *PLOS ONE* 8:e61548
69. Hinman F, ed. 1971. *Hydrodynamics of Micturition*. New York: Thomas
70. Yang PJ, Chen TG, Bracher SB, Hui A, Hu DL. 2023. Urinary flow through urethras with a rough lumen. *Neurourol. Urodyn.* 42:1245–54
71. Dass N, McMurray G, Greenland JE, Brading AF. 2001. Morphological aspects of the female pig bladder neck and urethra: quantitative analysis using computer assisted 3-dimensional reconstructions. *J. Urol.* 165:1294–99
72. Wheeler AP, Morad S, Buchholz N, Knight MM. 2012. The shape of the urine stream—from biophysics to diagnostics. *PLOS ONE* 7:e47133
73. Kjeld M. 2003. Salt and water balance of modern baleen whales: rate of urine production and food intake. *Can. J. Zool.* 81:606–16
74. Brodie C. 2006. Watch and learn: Benchwarming pays off for the archer fish. *Am. Sci.* 94:218–19
75. Davis BD, Dill L. 2012. Intraspecific kleptoparasitism and counter-tactics in the archerfish (*Toxotes chatareus*). *Behaviour* 149:1367–94

76. Gerullis P, Schuster S. 2014. Archerfish actively control the hydrodynamics of their jets. *Curr. Biol.* 24:2156–60
77. Vailati A, Zinnato L, Cerbino R. 2012. How archer fish achieve a powerful impact: hydrodynamic instability of a pulsed jet in *Toxotes jaculatorix*. *PLOS ONE* 7:e47867
78. Heath JE. 1966. Venous shunts in the cephalic sinuses of horned lizards. *Physiol. Zool.* 39:30–35
79. Sherbrooke WC, Middendorf GA III. 2001. Blood-squirting variability in horned lizards (*Phrynosoma*). *Copeia* 2001:1114–22
80. Middendorf GA III, Sherbrooke WC. 1992. Canid elicitation of blood-squirting in a horned lizard (*Phrynosoma cornutum*). *Copeia* 1992:519–27
81. Singh S. 2016. Guttation: mechanism, momentum and modulation. *Bot. Rev.* 82:149–82
82. Singh S. 2014. Guttation: new insights into agricultural implications. *Adv. Agron.* 128:97–135
83. Cerutti A, Jauneau A, Laufs P, Leonhardt N, Schattat MH, et al. 2019. Mangroves in the leaves: anatomy, physiology, and immunity of epithelial hydathodes. *Annu. Rev. Phytopathol.* 57:91–116
84. Gelstein S, Yeshurun Y, Rozenkrantz L, Shushan S, Frumin I, et al. 2011. Human tears contain a chemosignal. *Science* 331:226–30
85. Rühs PA, Bergfreund J, Bertsch P, Gstöhl SJ, Fischer P. 2021. Complex fluids in animal survival strategies. *Soft Matter* 17:3022–36
86. Boys CV. 1959. *Soap Bubbles and the Forces which Mould Them*, Science Study Ser. 3. New York: Anchor Doubleday Books
87. Bhat PP, Appathurai S, Harris MT, Pasquali M, McKinley GH, Basaran OA. 2010. Formation of beads-on-a-string structures during break-up of viscoelastic filaments. *Nat. Phys.* 6:625–31
88. Poole R. 2012. The Deborah and Weissenberg numbers. *Rheol. Bull.* 53:32–39
89. Dealy J. 2010. Weissenberg and Deborah numbers—their definition and use. *Rheol. Bull.* 79:14–18
90. Gaume L, Forterre Y. 2007. A viscoelastic deadly fluid in carnivorous pitcher plants. *PLOS ONE* 2:e1185
91. Zintzen V, Roberts CD, Anderson MJ, Stewart AL, Struthers CD, Harvey ES. 2011. Hagfish predatory behaviour and slime defence mechanism. *Sci. Rep.* 1:131
92. Concha A, Mellado P, Morera-Brenes B, Sampaio Costa C, Mahadevan L, Monge-Nájera J. 2015. Oscillation of the velvet worm slime jet by passive hydrodynamic instability. *Nat. Commun.* 6:6292
93. Gilbert C, Rayor LS. 1985. Predatory behavior of spitting spiders (Araneae: Scytodidae) and the evolution of prey wrapping. *J. Arachnol.* 13:231–41
94. Morera-Brenes B, Monge-Nájera J. 2010. A new giant species of placented worm and the mechanism by which onychophorans weave their nets (Onychophora: Peripatidae). *Rev. Biol. Trop.* 58:1127–42
95. Baer A, Schmidt S, Haensch S, Eder M, Mayer G, Harrington MJ. 2017. Mechanoresponsive lipid-protein nanoglobules facilitate reversible fibre formation in velvet worm slime. *Nat. Commun.* 8:974
96. Suter RB, Stratton GE. 2009. Spitting performance parameters and their biomechanical implications in the spitting spider, *Scytodes thoracica*. *J. Insect Sci.* 9:62
97. Bush JW, Hu DL. 2006. Walking on water: biolocomotion at the interface. *Annu. Rev. Fluid Mech.* 38:339–69
98. Suter RB, Stratton GE. 2005. *Scytodes* versus *Schizocosma* predatory techniques and their morphological correlates. *J. Arachnol.* 33:7–15
99. Ewoldt RH, Clasen C, Hosoi AE, McKinley GH. 2007. Rheological fingerprinting of gastropod pedal mucus and synthetic complex fluids for biomimicking adhesive locomotion. *Soft Matter* 3:634–43
100. Denny M. 1980. The role of gastropod pedal mucus in locomotion. *Nature* 285:160–61
101. Parker G. 1911. The mechanism of locomotion in gastropods. *J. Morphol.* 22:155–70
102. Lai JH, del Alamo JC, Rodríguez-Rodríguez J, Lasheras JC. 2010. The mechanics of the adhesive locomotion of terrestrial gastropods. *J. Exp. Biol.* 213:3920–33
103. Campion M. 1961. The structure and function of the cutaneous glands in *Helix aspersa*. *J. Cell Sci.* 3:195–216
104. Martini FH. 1998. The ecology of hagfishes. In *The Biology of Hagfishes*, ed. JM Jørgensen, JP Lomholt, RE Weber, H Malte, pp. 57–77. Dordrecht, Neth.: Springer
105. Böni L, Fischer P, Böcker L, Kuster S, Rühs PA. 2016. Hagfish slime and mucin flow properties and their implications for defense. *Sci. Rep.* 6:30371

106. Ewoldt RH, Winegard TM, Fudge DS. 2011. Non-linear viscoelasticity of hagfish slime. *Int. J. Nonlinear Mech.* 46:627–36
107. MacMinn CW. 2005. *The design and construction of a novel pipe flow apparatus for exploring polymer drug reduction*. PhD Thesis, Mass. Inst. Technol.
108. Gaume L, Forterre Y. 2007. A viscoelastic deadly fluid in carnivorous pitcher plants. *PLOS ONE* 2:e1185
109. Kang V, Isermann H, Sharma S, Wilson DI, Federle W. 2021. How a sticky fluid facilitates prey retention in a carnivorous pitcher plant (*Nepenthes rafflesiana*). *Acta Biomater.* 128:357–69
110. Vogel S. 2014. *Comparative Biomechanics: Life's Physical World*. Princeton, NJ: Princeton Univ. Press
111. Gosline JM, DeMont ME. 1985. Jet-propelled swimming in squids. *Sci. Am.* 252:96–103
112. Johnson W, Soden P, Trueman E. 1972. A study in jet propulsion: an analysis of the motion of the squid, *Loligo vulgaris*. *J. Exp. Biol.* 56:155–65
113. Krueger PS, Gharib M. 2003. The significance of vortex ring formation to the impulse and thrust of a starting jet. *Phys. Fluids* 15:1271–81
114. Vogel S. 1987. Flow-assisted mantle cavity refilling in jetting squid. *Biol. Bull.* 172:61–68
115. Zhu Q, Xiao Q. 2022. Physics and applications of squid-inspired jetting. *Bioinspirat. Biomimet.* 17:041001
116. Ward DV, Wainwright SA. 1972. Locomotory aspects of squid mantle structure. *J. Zool.* 167:437–49
117. Sutherland KR, Madin LP. 2010. Comparative jet wake structure and swimming performance of salps. *J. Exp. Biol.* 213:2967–75
118. Roh C, Gharib M. 2018. Asymmetry in the jet opening: underwater jet vectoring mechanism by dragonfly larvae. *Bioinspirat. Biomimet.* 13:046007
119. Mill P, Pickard R. 1975. Jet-propulsion in anisopteran dragonfly larvae. *J. Comp. Physiol.* 97:329–38
120. Linsenmair KE, Jander R. 1963. Das “Entspannungsschwimmen” von *Velia* und *Stenus*. *Naturwissenschaften* 50:231
121. Bush JW, Hu DL, Prakash M. 2007. The integument of water-walking arthropods: form and function. *Adv. Insect Physiol.* 34:117–92
122. Schildknecht H. 1976. Chemical ecology—a chapter of modern natural products chemistry. *Angew. Chem. Int. Ed. Engl.* 15:214–22
123. Nachtigall W. 1985. Swimming in aquatic insects. *Compr. Insect Physiol. Biochem. Pharmacol.* 5:467–90
124. Scharfman B, Techet A, Bush J, Bourouiba L. 2016. Visualization of sneeze ejecta: steps of fluid fragmentation leading to respiratory droplets. *Exp. Fluids* 57:24
125. Bourouiba L. 2021. The fluid dynamics of disease transmission. *Annu. Rev. Fluid Mech.* 53:473–508
126. Han M, Ooka R, Kikumoto H, Oh W, Bu Y, Hu S. 2021. Experimental measurements of airflow features and velocity distribution exhaled from sneeze and speech using particle image velocimetry. *Build. Environ.* 205:108293
127. Nunes J, Tsai S, Wan J, Stone HA. 2013. Dripping and jetting in microfluidic multiphase flows applied to particle and fibre synthesis. *J. Phys. D* 46:114002
128. Fahlman A, Loring SH, Levine G, Rocho-Levine J, Austin T, Brodsky M. 2015. Lung mechanics and pulmonary function testing in cetaceans. *J. Exp. Biol.* 218:2030–38
129. Barton C. 2020. *Characterization of the impulsive jet produced from a dolphin's blowhole*. PhD Thesis, Okla. State Univ.
130. Ngo A, Ford M, Barton C, Gaeta R, Jacob J. 2019. *Flow visualization of a dolphin blowhole*. Video presented at the 72nd Annual Meeting of the APS Division of Fluid Dynamics, Nov. 23. <https://doi.org/10.1103/APS.DFD.2019.GFM.V0060>.
131. Stockan JA, Robinson EJ. 2016. *Wood Ant Ecology and Conservation*. Cambridge, UK: Cambridge Univ. Press
132. Dean J, Aneshansley DJ, Edgerton HE, Eisner T. 1990. Defensive spray of the bombardier beetle: a biological pulse jet. *Science* 248:1219–21
133. Arndt EM, Moore W, Lee WK, Ortiz C. 2015. Mechanistic origins of bombardier beetle (Brachinini) explosion-induced defensive spray pulsation. *Science* 348:563–67
134. Eisner T. 1965. Defensive spray of a phasmid insect. *Science* 148:966–68
135. Meinwald J, Chadha M, Hurst J, Eisner I. 1962. Defense mechanisms of arthropods-IX Anisomorphal, the secretion of a phasmid insect. *Tetrahedron Lett.* 3:29–33

136. Eisner T, Aneshansley DJ. 1982. Spray aiming in bombardier beetles: jet deflection by the Coanda effect. *Science* 215:83–85
137. Woodburne RT, Lapides J. 1972. The ureteral lumen during peristalsis. *Am. J. Anat.* 133:255–58
138. Concha A, Mellado P, Morera-Brenes B, Sampaio Costa C, Mahadevan L, Monge-Nájera J. 2015. Oscillation of the velvet worm slime jet by passive hydrodynamic instability. *Nat. Commun.* 6:6292
139. Marmottant P, Villermaux E. 2004. On spray formation. *J. Fluid Mech.* 498:73–111
140. Mortensen NA, Okkels F, Bruus H. 2005. Reexamination of Hagen-Poiseuille flow: shape dependence of the hydraulic resistance in microchannels. *Phys. Rev. E* 71:057301
141. Chen HH, Brenner MP. 2004. The optimal faucet. *Phys. Rev. Lett.* 92:166106
142. Ward TA, Rezadad M, Fearday CJ, Viyapuri R. 2015. A review of biomimetic air vehicle research: 1984–2014. *Int. J. Micro Air Veh.* 7:375–94
143. Wang L, Hui Y, Fu C, Wang Z, Zhang M, Zhang T. 2020. Recent advances in gecko-inspired adhesive materials and application. *J. Adhesion Sci. Technol.* 34:2275–91
144. Zhang X, Shi F, Niu J, Jiang Y, Wang Z. 2008. Superhydrophobic surfaces: from structural control to functional application. *J. Mater. Chem.* 18:621–33
145. Zadesky SP, Rothkopf FR, Fletcher AE. 2016. *Liquid expulsion from an orifice*. US Patent 9,451,354
146. Xu NW. 2021. Squid-inspired robots perform swimmingly. *Sci. Robot.* 6:eabf4301
147. Rohilla P, Rane YS, Lawal I, Le Blanc A, Davis J, et al. 2019. Characterization of jets for impulsively-started needle-free jet injectors: influence of fluid properties. *J. Drug Deliv. Sci. Technol.* 53:101167
148. Bujard T, Giorgio-Serchi F, Weymouth GD. 2021. A resonant squid-inspired robot unlocks biological propulsive efficiency. *Sci. Robot.* 6:eabd2971
149. Christianson C, Cui Y, Ishida M, Bi X, Zhu Q, et al. 2020. Cephalopod-inspired robot capable of cyclic jet propulsion through shape change. *Bioinspirat. Biomimet.* 16:016014
150. Weymouth G, Subramaniam V, Triantafyllou M. 2015. Ultra-fast escape maneuver of an octopus-inspired robot. *Bioinspirat. Biomimet.* 10:016016
151. Booth A, McIntosh A, Beheshti N, Walker R, Larsson L, Copestake A. 2012. Spray technologies inspired by bombardier beetle. In *Encyclopedia of Nanotechnology*, ed. B Bhushan, pp. 2495–503. Dordrecht, Neth.: Springer